

## RESEARCH ARTICLE

 OPEN ACCESS

# Studying the Effect of Parasite Switching in Optimal Control Analysis of Sleeping Sickness

Mulalo Makhuvha<sup>a,b</sup> Hermane Mambili-Mamboundou<sup>a</sup><sup>a</sup>University of Kwazulu-Natal, South Africa; <sup>b</sup>DSI-NRF Centre of Excellence in Mathematical and Statistical Sciences (CoE-MaSS), South Africa

## ABSTRACT

We construct and analyze an immunological mathematical model to explore within-host dynamics of a neglected tropical vector disease called human African trypanosomiasis (HAT). The disease, caused by a parasite with immune-evading strategies, is represented by six differential equations encompassing type 1 and type 2 parasites, naive macrophages, classical macrophages, alternative activated macrophages, and cytokines. Initial analysis without control measures reveals a disease-free equilibrium and two endemic equilibria, one with co-existing type 1 and type 2 parasites and the other with only one parasite type. Additionally, we explore the impact of control measures on parasite persistence and extinction. Two optimal control models assess the effect of two therapeutic drugs; one focuses on the parasite's invasion, and the other targets the parasite growth rate. Findings indicate that the first drug shifts the system from co-existence to a type 2 parasite endemic state, while the growth inhibitor drug eliminates the parasite from the host.

## ARTICLE HISTORY

Received September 6, 2022  
Accepted August 30, 2023

## KEYWORDS

Immunology, Cytokines,  
Macrophages,  
Parasite Infection, Switching,  
Optimal Control

## 1 Introduction

Human African trypanosomiasis (HAT) also known as the sleeping sickness is one of the neglected tropical diseases transmitted by tsetse flies. The HAT disease is caused by a parasite named *Trypanosoma brucei*. There are two types of *Trypanosoma brucei* that cause the HAT disease, namely *Trypanosoma Brucei Gambiense* (TBG) and *Trypanosoma Brucei Rhodesiense* (TBR) (WHO, 2019). TBG causes the chronic form of the HAT disease, and TBR causes the acute form.

The World Health Organisation (WHO) had targets to have HAT disease eliminated by 2020, unfortunately, that has not been achieved because at the moment HAT is not of high importance to the WHO as compared to other diseases (WHO, 2019). HAT affects people in 36 countries in sub-Saharan Africa with 62% of the reported cases most predominately in Democratic Republic of Congo (Uniting to Combat NTD, 2019). In addition, TBG accounts for 80% of the reported cases.

HAT is complex to diagnose, and surveillance is difficult due to the fact that most of the people affected reside in remote rural places. The HAT disease harbour itself in both human and nonhuman hosts like cattle and wild animals, making it difficult to control as it requires different host to maintain itself into the community (Wamwiri et al., 2007). The disease being mostly chronic adds more strain to diagnoses, the infected individuals show mild symptoms in the first stage making it difficult to detect from case to case which can lead to the disease being fatal if not diagnosed early. The common symptoms in the first stage entail fever, headache, enlarged lymph nodes, joint pains, and itching (WHO, 2019). The more obvious signs and symptoms appear in the second stage when the parasite crosses the blood-brain barrier, affecting the central nervous system which causes changes in behavior, confusion, sensory disturbances, poor coordination, and sleeping disorder.

HAT is transmitted to humans by a bite from tsetse flies. During the biting, metacyclic trypomastigotes larvae get injected into the human host and later evolve into bloodstream trypomastigotes to easily be transported from the bloodstream to other organs. Once in the bloodstream, the parasites invade the immune system by antigenic variations of the glycoproteins surface coating (Rogers, 1988). Antigenic variation is the ability to switch periodically to thousands more parasite types. The HAT parasite is known to display extreme adaptation to their environment, therefore, the immune cells fail to identify the parasite once it has gone through that variation. The more they switch, the less the immune cells is able to keep up with the parasite leading to an increase in the parasite load.



The first line of defense against the trypanomastigotes are macrophages. Macrophages are an important part of the immune system for its function to engulf foreign substances, they are also responsible for the secretion of cytokines which plays an important role in the communication between immune cells during infections. In this study, we will consider three types of macrophages: the naive macrophages, the classical activated macrophages, and the alternative activated macrophages. Naive macrophages are made in the bone marrow and mature either into classical macrophages to form part of the innate immune system or, later on, into alternative activated macrophages to be part of the adaptive immune response. Innate immune response is initiated when a foreign substance enters the body, and it's mostly dealt with in a matter of a few hours. On the other hand, adaptive immune response takes over when the innate immune system is not able to destroy the invader.

For effective immune response, communication between various immune cells type is capital. At the center of that communication are chemical messengers called cytokines. Cytokines are proteins that bind to specific receptors to promote and activate immune cells (Turner et al., 2014). Their role is modulation of inflammation with TNF, NO, IL-1, IL-6, and IFN being pro-inflammatory signaling cytokines, IL-4 and IL-10 being the anti-inflammatory signaling cytokines. The pro-inflammation cytokines are responsible for enhancing and stimulating inflammatory responses whereas anti-inflammatory control the pro-inflammatory cytokine responses (Zhang and An, 2007). Cytokines are communication mediators. They alert the immune system when a response is needed. For the purposes of this study, cytokines will be considered collectively as part of their communication function in the human host.

The infection dynamics of HAT is still not well understood. Only a few noticeable mathematical models have been dedicated to studying this neglected tropical disease. This is mostly due to the fact that HAT has not enjoyed the attention given to more widespread disease like Cancer, HIV/AIDS, and Ebola. With those few noticeable HAT models most of them are population models (see, for example, Rogers, 1988; Ndong et al., 2016; Artzrouni and Gouteux, 1996; Gervas et al., 2018; Rock et al., 2015, to mention a few). Modeling African trypanosomiasis goes back to Rogers (1988) who presented a two-vertebrate-host species and one-vector species to simulate how the disease cannot be maintained by the human hosts alone. He had modified a model describing Malaria to allow for incubation and temporary immunity periods for both host species. Rogers also looked at the probability of transmission with a susceptible vector bites an infectious host. Results show that the disease prevalence can be influenced by fly density and seasonal changes in fly numbers. Unlike Rogers, Artzrouni and Gouteux (1996) considered modeling the disease with only the human as the main host for the parasite. From that paper we gather that the human host cannot be neglected since it plays a vital role in the HAT disease dynamics, and it is important to explicitly understand how the disease manifest in the human host.

With HAT being a vector borne disease, a study done by Ndong et al. (2016) models the transmission dynamics, taking into account the growth of the tsetse fly population at the different stages of its life cycle. That gave motivation to this study to take into account the different stages of the parasite life cycle and the different components involved in the disease transmission within the human host. Some studies modeled HAT by incorporating control theory in implementing measures like education, treatment, and insecticides to mathematical models (Gervas et al., 2018; Rock et al., 2015).

With population models being enhanced, less attention is paid to within-host models. It is imperative to focus attention on how within-host dynamics influence disease progression because diseases succeed when host mechanisms fail. Studying those mechanisms will lead to targeted control measures that can be implemented at the correct level of disease progression. An interesting study by Navarrete (2019) constructed a within-host mathematical model that associated host rhythms in temperature and immunity with parasite replication and immune evasion. Their findings show that temperature and immunity play an important role in mammal host transmission. Another within host model done by Frank (1999) developed a mathematical model that integrate parasite and host immunity, the results show that the minor modifications of switch rates by natural selection are required to develop a sequence of ordered parasites. The study does acknowledge that the switching rate can lead to a series of outbreaks that enable the parasite to escape immune surveillance.

There is little to no knowledge on the effect of antigenic variations by the parasite in evading the immune system within the human host. To our knowledge, there is no study that incorporate cytokines into the modeling of HAT. It is unrealistic to have immune cells singly working without incorporating the role of cytokines. This study seeks to investigate the effect of parasite switching in the evolution of the disease and how the immune system responds to the evasion. Our study differentiates the parasite types and acknowledges the specific immune response to the new parasite type. We later introduce treatment dynamics of different therapeutic drugs to capture the desirable effects of the drugs and expose the effects of drug toxicity. We employ optimal control theory to the improved models in order to get a desired outcome by optimising the duration of the infection while minimising the parasite in the system.

The paper is organised as follows: In Section 2, we introduce our immunological model. In Section 3, we present the mathematical analysis of the immunological model, which includes the positivity and uniqueness of solutions, model equilibria, and the stability of the model equilibria. In Section 4, we present the numerical solutions for the model; whereas, in Section 5, the optimal control models are analysed by incorporating effects of two different therapeutic drugs to the previous model. Moreover, the numerical simulations for the optimal control models are also presented in this section together with the optimality conditions solutions. Lastly, we provide the conclusion in Section 6.

## 2 Model Formulation

In this section, the basic immunological mathematical model that captures explicitly how the trypanosomiasis parasite interact with the immune system is developed. The within-host transmission is modeled using six variables: Parasite type 1  $P_1$ , Naive macrophages  $M_n$ , Classical activated macrophages  $M_c$ , Cytokine  $C$ , Alternative activation macrophages  $M_{aa}$ , and Parasite type 2  $P_2$ . The parameters and variables are explained in Tables 1 and 2, respectively.

From the model diagram in Figure 1, the following system of differential equations are derived:

$$\frac{dP_1}{dt} = \alpha_1 P_1 - s_1 P_1 - k_1 P_1 M_c - \mu_1 P_1, \quad (1)$$

$$\frac{dM_n}{dt} = \Lambda_n - \alpha_n M_n P_1 + (1 - k_1) P_1 M_c + (1 - k_2) P_2 M_{aa} - \alpha_c M_n - \alpha_{aa} M_n P_2 + \alpha_I M_n C - \mu_n M_n, \quad (2)$$

$$\frac{dM_c}{dt} = \alpha_n M_n P_1 + \alpha_c M_n + \gamma_c M_c C - (1 - k_1) P_1 M_c - \mu_c M_c, \quad (3)$$

$$\frac{dM_{aa}}{dt} = \alpha_{aa} M_n P_2 + \gamma_{aa} M_{aa} C - (1 - k_2) P_2 M_{aa} - \mu_{aa} M_{aa}, \quad (4)$$

$$\frac{dC}{dt} = \alpha_{p1} P_1 M_c + \alpha_{p2} P_2 M_{aa} - \alpha_I M_n C - \gamma_{aa} M_{aa} C - \gamma_c M_c C - \mu_s C, \quad (5)$$

$$\frac{dP_2}{dt} = s_1 P_1 + \alpha_2 P_2 - k_2 P_2 M_{aa} - \mu_2 P_2. \quad (6)$$

Equation (1) describes the rate of change of parasite type 1 over time, the equation was developed considering the different mechanism in the parasite population growth, switching to another type and removal. The recruited parasites multiply through binary fusion that follows exponential growth with the growth rate given by  $\alpha_1$ . The second term in Equation (1) models the parasite switches at a switch rate  $s_1$  (Frank, 1999). Switching to more parasite types can be easily incorporated despite our restriction on parasite types. The third term models the parasite being engulfed by classical macrophages at a rate  $k_1$ . It is assumed that parasite type 1 population decays at a natural rate  $\mu_1$ .

Equation (2) describes the rate of change of the naive macrophages over time. In addition to the immune system, this population is affected by deactivated macrophages and macrophage activation. The first term of the Equation (2) models the recruitment of the naive macrophages at a rate  $\Lambda_n$ . The second term of the Equation (2) represents naive macrophages being activated by dead parasite by a process called classical activation (Baral, 2010). The third and fourth term models the deactivation of the classical and alternative activated macrophages when they interact with the parasites. The fifth and sixth terms describe the differentiation of the naive macrophages into classical and alternative activated macrophages, respectively (Rőszer, 2015). When cytokines bind to then naive macrophages more of the macrophages are produced at a rate  $\alpha_I$ . It is assumed that this population decays naturally at a  $\mu_n$ .

Equation (3) describe the rate of change of the classical activated macrophages over time. The naive macrophages activated by dead parasites increase the classical macrophages population, this is modeled by the first term of Equation (3). As a result of differentiation of naive macrophages, the classical macrophage population is supplied with more classical macrophages at an activation rate  $\alpha_c$ . Similarly to naive macrophages, more classical macrophages are produced at the rate  $\gamma_c$  when they bind to the cytokines. When classical activated macrophages come into contact with parasites, they deactivate to naive macrophages at a rate of  $(1 - k_1)$ , reducing the population of this macrophage. It is assumed that the classical macrophages decay naturally at a rate  $\mu_c$ .

Equation (4) describe the rate of change of the alternative activated macrophages with respect to time. In the presence of parasite type 2, these macrophages activate in order to combat infection (Rőszer, 2015). The alternative activated macrophages are produced when naive macrophages differentiate, at an activation rate of  $\gamma_{aa}$ . In the third term model the deactivated  $M_{aa}$  macrophages when they interact with the parasite type 2. The population of alternative activation macrophages is assumed to decay naturally at a rate  $\mu_{aa}$ .

Equation (5) describe the rate of change of the concentration of a group of cytokines over time. Macrophages secrete cytokines, which are represented by the parameters  $\alpha_{p1}$ ,  $\alpha_{p2}$ . The cytokines are responsible for the activation of the three types of macrophages which in turn reduces the concentration of the  $C$  at a rate  $\alpha_c$ ,  $\gamma_{aa}$ , and  $\gamma_c$ . With the disease progressing, the concentration of cytokine is assumed to decay naturally at a rate  $\mu_s$ .

Equation (6) describes the rate of change of parasite type 2 with respect to time. Equation (6) is developed following the parasite switch, growth, and removal. The first term of the equation (6) models the parasite switch from first type to the second type of parasite. Similarly to type 1 parasite, the second type grow exponentially. The third term represents the killing effect of alternative activated macrophages on type 2 parasite at a rate  $k_2$ . It is assumed that parasite type 2 decay naturally at a rate  $\mu_2$ .

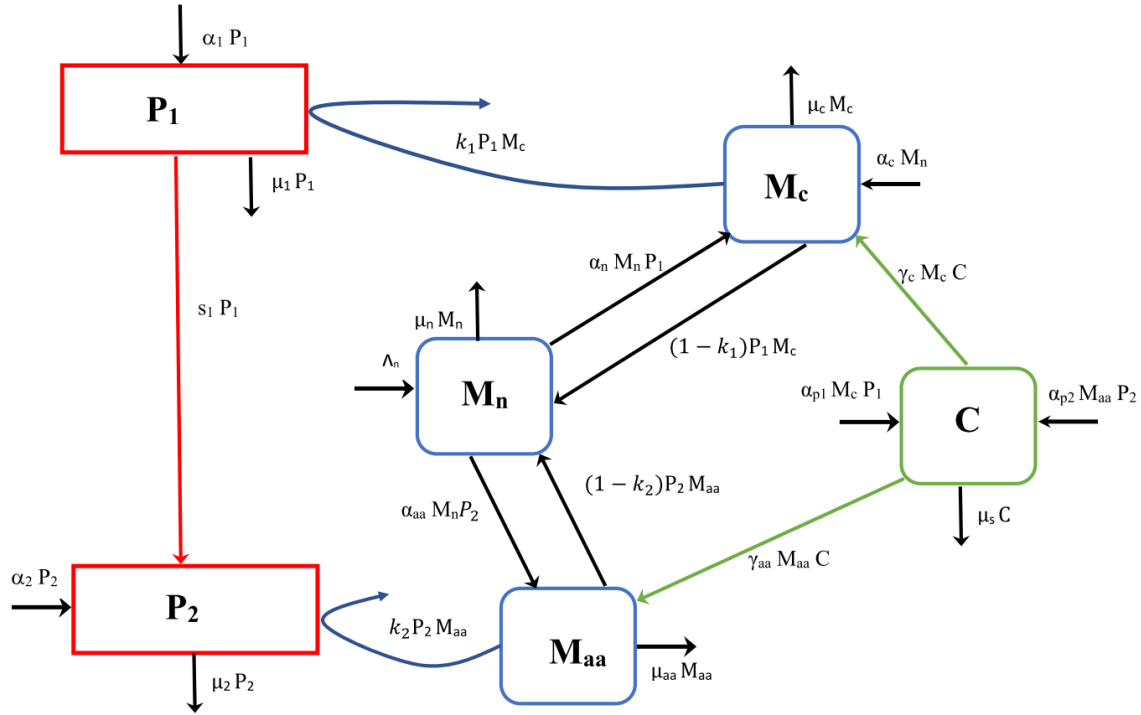


**Figure 1:** HAT immunological transmission dynamics.

**Table 1:** Description of the parameters of the model.

Parameter	Description
$\alpha_1$	Growth rate of parasite type 1
$s_1$	Switching rate of the parasite type 1 to parasite type 2
$k_1$	Killing rate of parasite type 1 by classical macrophages
$\mu_1$	Natural death rate of the parasite type 1
$\Lambda_n$	Supply of naive macrophages
$\alpha_n$	Activation rate of naive macrophages by dead parasite
$\alpha_c$	Activation rate of the classical macrophages from the naive macrophages
$\alpha_{aa}$	Activation rate of the alternative activated macrophages from naive macrophages
$\alpha_l$	Activation rate of naive macrophages by cytokine
$\mu_n$	Natural death rate of naive macrophages
$\gamma_c$	Production rate for classical macrophages in the presence of cytokine
$\mu_c$	Natural death rate of classical macrophages
$\gamma_{aa}$	Activation of alternative activated macrophages by the presence of cytokines
$\mu_s$	Natural decay of cytokines
$\alpha_{p1}$	Secretion rate of cytokine by classical macrophages
$\alpha_{p2}$	Secretion rate of cytokine by the alternative activated macrophages
$k_2$	Killing rate of parasite type 2 by alternative activated macrophages
$\mu_{aa}$	Natural death rate of the alternative activated macrophages
$\alpha_2$	Growth rate of parasite type 2
$\mu_2$	Natural death rate of parasite type 2

**Table 2:** Description of the state variables of the model.

Variables	Description	Initial Value
$P_1(t)$	Parasite type 1 population size	1000
$M_n(t)$	Naive macrophage population size	800
$M_c(t)$	Classical macrophage population size	500
$M_{aa}(t)$	Alternative activated macrophage population size	0
$C$	Cytokine population size	3.8
$P_2(t)$	Parasite type 2 population size	0

### 3 Mathematical Analysis

In this section, we show that the solutions to the system of equations (1)–(6) exist and are unique, and that the solutions remain positive for all time  $t \geq 0$ . In addition, the system's equilibria is given together with the stability analysis of both the disease-free equilibrium and endemic equilibrium.

#### 3.1 Existence and uniqueness of solutions

We need to prove existence and uniqueness of the solutions for the system of equations (1)–(6). To show uniqueness, the system of equations can be written in the form  $x' = H(x)$  with  $x = (P_1, M_n, M_c, M_{aa}, C, P_2)$  and re-indexing  $x = (x_1, x_2, x_3, x_4, x_5, x_6)$ . Therefore, we define

$$\begin{aligned} H_1(x) &= \alpha_1 x_1 - s_1 x_1 - k_1 x_1 x_2 - \mu_1 x_1, \\ H_2(x) &= \Lambda_n - \alpha_n x_2 x_1 + (1 - k_1) x_1 x_3 + (1 - k_2) x_6 x_4 - \alpha_c x_2 - \alpha_{aa} x_2 x_6 + \alpha_I x_2 x_5 - \mu_n x_2, \\ H_3(x) &= \alpha_n x_2 x_1 + \alpha_c x_2 + \gamma_c x_3 x_5 - (1 - k_1) x_1 x_3 - \mu_c x_3, \\ H_4(x) &= \alpha_{aa} x_2 x_6 + \gamma_{aa} x_4 x_5 - (1 - k_2) x_6 x_4 - \mu_{aa} x_4, \\ H_5(x) &= \alpha_{p1} x_1 x_3 + \alpha_{p2} x_6 x_4 - \alpha_I x_2 x_5 - \gamma_{aa} x_4 x_5 - \gamma_c x_3 x_5 - \mu_s x_5, \\ H_6(x) &= s_1 x_1 + \alpha_2 x_6 - k_2 x_6 x_4 - \mu_2 x_6. \end{aligned}$$

**Theorem 3.1** (see Thieme, 1948, Theorem A.4). *Let  $\mathbb{R}_+^n = [0, \infty)^n$  be the cone of non-negative vector in  $\mathbb{R}_+^n$ . Let  $H: \mathbb{R}_+^{n+1} \rightarrow \mathbb{R}_+^n$  be a Lipschitz function,  $H(t, x) = (H_1(t, x), H_2(t, x), \dots, H_6(t, x))$  satisfying  $H_i(t, x) \geq 0$  whenever  $t \geq 0$ ,  $x \in \mathbb{R}_+^n$ ,  $x_i = 0$ . Then, for every  $x^0 \in \mathbb{R}_+^n$ , there exists a unique solution of  $x' = H(t, x)$ ,  $x(0) = x^0$ , with values in  $\mathbb{R}_+^n$ , which is defined on some time interval  $[0, b)$ ;  $b > 0$ .*

Using Theorem 3.1 we then check for  $i = 1, 2, 3, 4, 5, 6$ ,  $H_i(x) \geq 0$  if  $x \in \mathbb{R}_+^6$  and  $x_i = 0$ ; therefore,

$$\begin{aligned} H_1(0, M_n, M_c, M_{aa}, C, P_2) &= 0, \\ H_2(P_1, 0, M_c, M_{aa}, C, P_2) &= \Lambda_n + (1 - k_1) P_1 M_c + (1 - k_2) P_2 M_{aa} \geq 0, \\ H_3(P_1, M_n, 0, M_{aa}, C, P_2) &= \alpha_n M_n P_1 + \alpha_c M_n \geq 0, \\ H_4(P_1, M_n, M_c, 0, C, P_2) &= \alpha_{aa} M_n P_2 \geq 0, \\ H_5(P_1, M_n, M_c, M_{aa}, 0, P_2) &= \alpha_{p1} P_1 M_c + \alpha_{p2} P_2 M_{aa} \geq 0, \\ H_6(P_1, M_n, M_c, M_{aa}, C, 0) &= 0. \end{aligned}$$

We can further define  $H(t, x) = H(t_+, x_+)$  where  $t_+ = \max\{t, 0\}$  and  $x_+ = (x_1, x_2, x_3, x_4, x_5, x_6)$  are positive parts of the scalar  $t$  and vector  $x$ . We can check that  $\|x_+ - y_+\| \leq \|x - y\|$  for any of the usual norms on  $\mathbb{R}^n$ . Hence  $H$  is a locally Lipschitz continuous vector field on  $\mathbb{R}^6$  satisfies  $H_i(t, x) \geq 0$  for all  $t \in \mathbb{R}$ ,  $x \in \mathbb{R}_+^6$ ,  $x_i = 0$ .

#### 3.2 Positivity of solutions

We need to prove that all the variables remain non-negative given positive initial conditions for all time  $t \geq 0$ .

**Lemma 3.2.** *Let the non-negative initial conditions be  $(P_1(0) \geq 0, M_n(0) \geq 0, M_c(0) \geq 0, M_{aa}(0) \geq 0, C(0) \geq 0, P_2(0) \geq 0) \in \mathbb{R}_+^6$ , then all solutions of the system of equations (1)–(6) are positive for all  $t > 0$  and non-negative for all  $t$  such that all positive solution satisfy  $(P_1(t) > 0, M_n(t) > 0, M_c(t) > 0, M_{aa}(t) > 0, C(t) > 0, P_2(t) > 0)$  for all large  $t$ .*

*Proof.* From the system of equations (1)–(6) we have the first equation as

$$\frac{dP_1}{dt} = \alpha_1 P_1 - s_1 P_1 - k_1 P_1 M_c - \mu_1 P_1.$$

We then obtain the inequality to be

$$\frac{dP_1}{dt} \geq -s_1 P_1 - k_1 P_1 M_c - \mu_1 P_1.$$

Then it follows that

$$\frac{dP_1}{dt} \geq (-s_1 - k_1 M_c - \mu_1) P_1 \quad \Rightarrow \quad \frac{dP_1}{P_1} \geq (-s_1 - k_1 M_c - \mu_1) dt.$$

Integrate the above expression

$$P_1(t) \geq P_1(0) \exp\left(-\left((s_1 + \mu_c)t + \int_0^t k_1 M_c(s) ds\right)\right).$$

Similarly, we have

$$\begin{aligned} M_n(t) &\geq M_n(0) \exp\left(-\left(\mu_n t + \int_0^t (\alpha_c P_1(s) ds + \alpha_{aa} P_2(s) ds)\right)\right), \\ M_c(t) &\geq M_c(0) \exp\left(-\left(\mu_c t + \int_0^t (1 - k_1) P_1(s) ds\right)\right), \\ C(t) &\geq C(0) \exp\left(-\left(\mu_s t + \int_0^t (\alpha_I M(s) ds + \gamma_c M_c(s) ds + \gamma_{aa} M_{aa}(s) ds)\right)\right), \\ M_{aa}(t) &\geq M_{aa}(0) \exp\left(-\left(\mu_{aa} t + \int_0^t (1 - k_2) P_2(s) ds\right)\right), \\ P_2(t) &\geq P_2(0) \exp\left(-\left(\mu_2 t + \int_0^t k_2 M_{aa}(s) ds\right)\right). \end{aligned}$$

It then follows that

$$\begin{aligned} \lim_{t \rightarrow \infty} P_1(t) &> 0, & \lim_{t \rightarrow \infty} M_n(t) &> 0, & \lim_{t \rightarrow \infty} M_c(t) &> 0, \\ \lim_{t \rightarrow \infty} C(t) &> 0, & \lim_{t \rightarrow \infty} M_{aa}(t) &> 0, & \lim_{t \rightarrow \infty} P_2(t) &> 0. \end{aligned}$$

Therefore, we can conclude that  $P_1(t), M_n(t), M_c(t), M_{aa}(t), C(t), P_2(t)$  are positive for all  $t > 0$  □

### 3.3 Model equilibria

In this subsection we give the model equilibrium states and the stability analysis of both the disease-free equilibrium and endemic equilibrium.

#### 3.3.1 Disease-free equilibrium (DFE)

The disease-free equilibrium is when there is no HAT disease in the human host. The equilibrium point is found by equating the right hand side of the system of equations (1)–(6) to zero, thus the DFE point is given by

$$E_0 = \left(0, \frac{\Lambda_n}{\alpha_c + \mu_n}, \frac{\alpha_c \Lambda_n}{\mu_c (\alpha_c + \mu_n)}, 0, 0, 0\right).$$

The DFE describes the natural immune response in the absence of parasites. Only naive macrophages and classical macrophages are present. Moreover, alternative activated macrophages are non-existent at the DFE, due to the fact that the adaptive immune response is not yet required.

#### 3.3.2 Endemic equilibrium (EE)

The endemic equilibrium point represents the state at which the disease persists in the human host. The solutions to the system of equations (1)–(6) reach the solution curves given by

$$E^* = (P_1^*, M_n^*, M_c^*, M_{aa}^*, C^*, P_2^*).$$

We found that there exist two endemic equilibrium points for the system of equations (1)–(6), which are as follows:

**Case 1:** There is no parasite  $P_1$ ; only parasite  $P_2$  exists. That is,  $P_1 = 0$  and only parasite  $P_2$  exists; therefore, the disease continues. In this scenario, the endemic point is given by

$$E_1^* = (0, M_n^*, M_c^*, M_{aa}^*, C^*, P_2^*)$$

where

$$\begin{aligned} P_1^* &= 0, \\ M_n^* &= -\frac{\alpha_2(\mu_{aa} - C^*\gamma_{aa}) + \mu_2(C^*\gamma_{aa} - \mu_{aa}) - k_2\Lambda_n}{k_2(\alpha_c - \alpha_i C^* + \mu_n)}, \\ M_c^* &= -\frac{\alpha_c(\alpha_2(C^*\gamma_{aa} - \mu_{aa}) + \mu_2(\mu_{aa} - C^*\gamma_{aa}) + k_2\Lambda_n)}{k_2(C^*\gamma_c - \mu_c)(\alpha_c - \alpha_i C^* + \mu_n)}, \\ M_{aa}^* &= \frac{\alpha_2 - \mu_2}{k_2}, \\ C^* &= \frac{P_2^* M_{aa}^* \alpha_{p2}}{\gamma_{aa} M_{aa}^* + \gamma_c M_c^* + \alpha_i M_n^* + \mu_s}, \\ P_2^* &= \frac{(\alpha_2 - \mu_2)(C^*\gamma_{aa} - \mu_{aa})(-\alpha_c + \alpha_i C^* - \mu_n)}{\mu_2 \alpha_{aa} \mu_{aa} + \alpha_2(\alpha_{aa}(C^*\gamma_{aa} - \mu_{aa}) + (k_2 - 1)\alpha_c + (k_2 - 1)\mu_n) - C^* \mu_2 \alpha_{aa} \gamma_{aa} + k_2 \alpha_{aa} \Lambda_n + e_0}, \end{aligned}$$

and where

$$e_0 = \mu_2 \alpha_c - k_2 \mu_2 \alpha_c - \alpha_i C^* (k_2 - 1) (\alpha_2 - \mu_2) - k_2 \mu_2 \mu_n + \mu_2 \mu_n.$$

**Case 2:** Both parasites  $P_1$  and  $P_2$  co-exist. In this scenario, the endemic point is given by

$$E_2^* = (P_1^{**}, M_n^{**}, M_c^{**}, M_{aa}^{**}, C^{**}, P_2^{**})$$

where

$$\begin{aligned} P_1^{**} &= \frac{(\mu_{aa} - C^{**}\gamma_{aa})(b_3) + P_2(b_1)}{(C^{**}\gamma_{aa} - \mu_{aa})(b_4) + P_2(b_2)}, \\ M_n^{**} &= \frac{((k_2 - 1)P_2^{**} + C^{**}\gamma_{aa} - \mu_{aa})(-k_1\Lambda_n + C^{**}\gamma_c\mu_1 + s_1(C^{**}\gamma_c - \mu_c) - \mu_1\mu_c + \alpha_1(\mu_c - C^{**}\gamma_c))}{k_1((C^{**}\gamma_{aa} - \mu_{aa})(C^{**}\alpha_i - \mu_n) + P_2^{**}(C^{**}(k_2 - 1)\alpha_i + \alpha_{aa}(\mu_{aa} - C^{**}\gamma_{aa}) - (k_2 - 1)\mu_n))}, \\ M_c^{**} &= \frac{\alpha_1 - s_1 - \mu_1}{k_1}, \\ M_{aa}^{**} &= \frac{P_2^{**}\alpha_{aa}(k_1\Lambda_n - C^{**}\gamma_c\mu_1 + \alpha_1(C^{**}\gamma_c - \mu_c) + \mu_1\mu_c + s_1(\mu_c - C^{**}\gamma_c))}{k_1((C^{**}\gamma_{aa} - \mu_{aa})(C^{**}\alpha_i - \mu_n) + P_2^{**}(C^{**}(k_2 - 1)\alpha_i + \alpha_{aa}(\mu_{aa} - C^{**}\gamma_{aa}) - (k_2 - 1)\mu_n))}, \\ C^{**} &= \frac{P_2^{**} M_{aa}^{**} \alpha_{p2} + P_1^{**} M_c^{**} \alpha_{p1}}{\gamma_{aa} M_{aa}^{**} + \gamma_c M_c^{**} + \alpha_i M_n^{**} + \mu_s}, \\ P_2^{**} &= \frac{P_1^{**} s_1}{k_2 M_{aa}^{**} - \alpha_2 - \mu_2}, \end{aligned}$$

and where

$$\begin{aligned} b_1 &= -\alpha_1 \alpha_{aa} \gamma_{aa} \gamma_c (C^{**})^2 + \alpha_{aa} \gamma_{aa} \gamma_c \mu_1 (C^{**})^2 - k_2 \alpha_1 \alpha_c \gamma_c C^{**} + \alpha_1 \alpha_c \gamma_c C^{**} + k_2 \alpha_c \gamma_c \mu_1 C^{**} - \alpha_c \gamma_c \mu_1 C^{**} \\ &\quad + \alpha_1 \alpha_{aa} \gamma_c \mu_{aa} C^{**} - \alpha_{aa} \gamma_c \mu_1 \mu_{aa} C^{**} + (k_2 - 1) \alpha_i (\alpha_1 - \mu_1) (C^{**} \gamma_c - \mu_c) C^{**} + \alpha_1 \alpha_{aa} \gamma_{aa} \mu_c C^{**} \\ &\quad - k_2 \alpha_1 \gamma_c \mu_n C^{**} + \alpha_1 \gamma_c \mu_n C^{**} + k_2 \gamma_c \mu_1 \mu_n C^{**} - \gamma_c \mu_1 \mu_n C^{**} + k_1 \alpha_c \Lambda_n - k_1 k_2 \alpha_c \Lambda_n + k_2 \alpha_1 \alpha_c \mu_c - \alpha_1 \alpha_c \mu_c \\ &\quad - k_2 \alpha_c \mu_1 \mu_c + \alpha_c \mu_1 \mu_c - \alpha_1 \alpha_{aa} \mu_{aa} \mu_c + \alpha_{aa} \mu_1 \mu_{aa} \mu_c + k_2 \alpha_1 \mu_c \mu_n - \alpha_1 \mu_c \mu_n - k_2 \mu_1 \mu_c \mu_n + \mu_1 \mu_c \mu_n \\ &\quad - s_1 (C^{**} \gamma_c - \mu_c) (C^{**} (k_2 - 1) \alpha_i - k_2 \alpha_c + \alpha_c - C^{**} \alpha_{aa} \gamma_{aa} + \alpha_{aa} \mu_{aa} - k_2 \mu_n + \mu_n) - \alpha_{aa} \gamma_{aa} \mu_1 \mu_c C^{**}, \\ b_2 &= -C^{**} \alpha_1 \alpha_{aa} \gamma_{aa} + C^{**} k_1 \alpha_1 \alpha_{aa} \gamma_{aa} + C^{**} \alpha_{aa} \mu_1 \gamma_{aa} - C^{**} k_1 \alpha_{aa} \mu_1 \gamma_{aa} - C^{**} \alpha_1 \alpha_n \gamma_c + C^{**} k_2 \alpha_1 \alpha_n \gamma_c - k_1 \alpha_n \Lambda_n \\ &\quad + k_1 k_2 \alpha_n \Lambda_n - C^{**} (k_1 - 1) (k_2 - 1) \alpha_i (\alpha_1 - \mu_1) + C \alpha_n \gamma_c \mu_1 - C^{**} k_2 \alpha_n \gamma_c \mu_1 - k_1 \alpha_1 \alpha_{aa} \mu_{aa} + \alpha_1 \alpha_{aa} \mu_{aa} \\ &\quad + k_1 \alpha_{aa} \mu_1 \mu_{aa} - \alpha_{aa} \mu_1 \mu_{aa} - k_2 \alpha_1 \alpha_n \mu_c + \alpha_1 \alpha_n \mu_c + k_2 \alpha_n \mu_1 \mu_c - \alpha_n \mu_1 \mu_c - k_1 \alpha_1 \mu_n + k_1 k_2 \alpha_1 \mu_n - k_2 \alpha_1 \mu_n \\ &\quad + k_1 \mu_1 \mu_n - k_1 k_2 \mu_1 \mu_n + k_2 \mu_1 \mu_n - \mu_1 \mu_n + \alpha_1 \mu_n \\ &\quad + s_1 (C^{**} (k_1 - 1) (k_2 - 1) \alpha_i - (k_1 - 1) \alpha_{aa} (C^{**} \gamma_{aa} - \mu_{aa}) - (k_2 - 1) (\alpha_n (C^{**} \gamma_c - \mu_c) + (k_1 - 1) \mu_n)), \end{aligned}$$

$$\begin{aligned}
 b_3 &= C^{**} \alpha_1 \alpha_c \gamma_c - C^{**} \alpha_c \mu_1 \gamma_c + C^{**} \alpha_1 \mu_n \gamma_c - C^{**} \mu_1 \mu_n \gamma_c + k_1 \alpha_c \Lambda_n - C^{**} \alpha_i (\alpha_1 - \mu_1) (C^{**} \gamma_c - \mu_c) - \alpha_1 \alpha_c \mu_c \\
 &\quad + \alpha_c \mu_1 \mu_c + s_1 (C^{**} \gamma_c - \mu_c) (C^{**} \alpha_i - \alpha_c - \mu_n) - \alpha_1 \mu_c \mu_n + \mu_1 \mu_c \mu_n, \\
 b_4 &= C^{**} \alpha_1 \alpha_n \gamma_c - C^{**} \alpha_n \mu_1 \gamma_c + k_1 \alpha_n \Lambda_n - C^{**} (k_1 - 1) \alpha_i (\alpha_1 - \mu_1) - \alpha_1 \alpha_n \mu_c + \alpha_n \mu_1 \mu_c + k_1 \alpha_1 \mu_n - \alpha_1 \mu_n \\
 &\quad - k_1 \mu_1 \mu_n + \mu_1 \mu_n + s_1 (C (k_1 - 1) \alpha_i + \alpha_n (\mu_c - C^{**} \gamma_c) - (k_1 - 1) \mu_n).
 \end{aligned}$$

### 3.4 Stability analysis of model equilibria

In this subsection, we focus on the stability analysis of the model equilibrium points of the system of equations (1)–(6).

#### 3.4.1 Local stability of the DFE

The stability of the disease free equilibrium point  $E_0$ , is determined by solving  $|J(E_0) - \lambda I| = 0$  where  $\lambda$  is the eigenvalue. According to van den Driessche and Watmough, if the eigenvalue of the Jacobian have negative real parts, then the point  $E_0$  is a locally asymptomatic stable. The Jacobian matrix associated with the system of equations (1)–(6) at  $E_0$  is given by

$$J(E_0) = \begin{pmatrix} \alpha_1 - k_1 M_c - \mu_1 - s_1 & 0 & 0 & 0 & 0 & 0 \\ (1 - k_1) M_c - M_n \alpha_n & -\alpha_c - \mu_n & 0 & 0 & \alpha_I M_n & -\alpha_{aa} M_n \\ M_n \alpha_n - (1 - k_1) M_c & \alpha_c & -\mu_c & 0 & \gamma_c M_c & 0 \\ 0 & 0 & 0 & -\mu_{aa} & 0 & \alpha_{aa} M_n \\ M_c \alpha_{p1} & 0 & 0 & 0 & -\gamma_c M_c - \alpha_I M_n - \mu_s & 0 \\ s_1 & 0 & 0 & 0 & 0 & \alpha_2 - \mu_2 \end{pmatrix}$$

where

$$M_n = \frac{\Lambda_n}{\alpha_c + \mu_n}, \quad M_c = \frac{\alpha_c \Lambda_n}{\mu_c (\alpha_c + \mu_n)}.$$

The eigenvalues for the above Jacobian matrix are given by

$$\begin{aligned}
 \lambda_1 &= \alpha_2 - \mu_2, \\
 \lambda_2 &= -\mu_{aa}, \\
 \lambda_3 &= -\mu_c, \\
 \lambda_4 &= -\alpha_c - \mu_n, \\
 \lambda_5 &= \frac{-(\mu_1 \alpha_c \mu_c - \alpha_1 \alpha_c \mu_c + k_1 \alpha_c \Lambda_n - \alpha_1 \mu_c \mu_n + \mu_1 \mu_c \mu_n + s_1 \mu_c \mu_n + s_1 \alpha_c \mu_c)}{\mu_c (\alpha_c + \mu_n)}, \\
 \lambda_6 &= \frac{-\alpha_c \gamma_c \Lambda_n - \alpha_i \mu_c \Lambda_n - \mu_c \mu_n \mu_s - \alpha_c \mu_c \mu_s}{\mu_c (\alpha_c + \mu_n)}.
 \end{aligned}$$

The eigenvalues  $\lambda_2, \lambda_3, \lambda_4$ , and  $\lambda_6$  have negative real parts. For  $\lambda_1$  and  $\lambda_5$  to have negative real parts, the following conditions have to hold:

$$\frac{\alpha_2}{\mu_2} < 1, \quad \frac{\alpha_1 \alpha_c \mu_c + \alpha_1 \mu_c \mu_n}{\mu_1 \alpha_c \mu_c + k_1 \alpha_c \Lambda_n + \mu_1 \mu_c \mu_n + s_1 \mu_c \mu_n + s_1 \alpha_c \mu_c} < 1. \tag{7}$$

To understand the biological meaning of these conditions, we observe that from Equation (6), when  $P_1 = 0$  at the DFE,  $P_2$  tends to be zero only when  $\alpha_2 < k_2 M_{aa} + \mu_2$  because  $k_2 M_{aa} + \mu_2$  is the rate at which  $P_2$  decreases overall and  $\alpha_2$  is  $P_2$ 's reproductive rate. Hence

$$\frac{\alpha_2}{\alpha_2 + k_2 M_{aa} + \mu_2} < 1.$$

This means that the reproductive rate of  $P_2$  should be less than the rate at which  $P_2$  is being washed out of the host. Since  $M_{aa} = 0$  at DFE, the condition reduces to  $\frac{\alpha_2}{\mu_2} < 1$ . The second condition on Equation (7) can be written as

$$\frac{\alpha_1}{\mu_1 + \frac{k_1 \alpha_c \Lambda_n}{\mu_c (\alpha_c + \mu_n)} + s_1} < 1$$

where  $M_c^*$  is the value of  $M_c$  at the DFE. Using the same reasoning, for  $P_1$  in Equation (1),  $P_1$  tends to zero only if  $\alpha_1 < \mu_1 + k_1 M_c^* + s_1$ , where  $\mu_c + K_1 M_c^* + s_1$  is the overall decreasing rate of  $P_1$ . Hence for the DFE to be stable, the reproduction rates of all parasite types should be less than their overall flashing rates.

### 3.4.2 Local stability of endemic equilibrium

The stability of the endemic point  $E_1^*$  depends on the stability of the Jacobian matrix  $J(E_1^*)$  given by

$$J(E_1^*) = \begin{pmatrix} L_0 & 0 & 0 & 0 & 0 & 0 \\ (1 - k_1)M_c^* - M_n^*\alpha_n & L_6 & 0 & (1 - k_2)P_2^* & \alpha_I M_n^* & (1 - k_2)M_{aa}^* - \alpha_{aa}M_n^* \\ M_n^*\alpha_n - (1 - k_1)M_c^* & \alpha_c & L_7 & 0 & \gamma_c M_c^* & 0 \\ 0 & \alpha_{aa}P_2^* & 0 & L_3 & \gamma_{aa}M_{aa}^* & \alpha_{aa}M_n^* - (1 - k_2)M_{aa}^* \\ \alpha_{p1}M_c^* & -\alpha_I C^* & -\gamma_c C^* & \alpha_{p2}P_2^* - \gamma_{aa}C^* & L_4 & \alpha_{p2}M_{aa}^* \\ s_1 & 0 & 0 & -k_2P_2^* & 0 & L_5 \end{pmatrix}$$

where

$$\begin{aligned} L_0 &= \alpha_1 - k_1M_c^* - \mu_1 - s_1, & L_3 &= \gamma_{aa}C^* - (1 - k_2)P_2^* - \mu_{aa}, & L_4 &= -\alpha_I M_n^* - \gamma_{aa}M_{aa}^* - \gamma_c M_c^* - \mu_s, \\ L_5 &= \alpha_2 - k_2M_{aa}^* - \mu_2, & L_6 &= \alpha_I C^* - \alpha_c - \alpha_{aa}P_2^* - \mu_n, & L_7 &= \gamma_c C^* - \mu_c. \end{aligned}$$

We find the sign of eigenvalues using the Gershgorian Circle Theorem below, where  $n = 6$ .

**Theorem 3.3** (Gershgorian theorem from Bejarano et al., 2018). *Let  $\bar{x}$  be an equilibrium point of a dynamical system in the form  $\frac{dx}{dt} = f(x)$ ,*

$$Df(\bar{x}) = \begin{pmatrix} J_{11} & J_{12} & \cdots & J_{1n} \\ J_{21} & J_{22} & \cdots & J_{2n} \\ \vdots & \vdots & \ddots & \vdots \\ J_{n1} & J_{n2} & \cdots & J_{nn} \end{pmatrix}$$

*the Jacobian matrix of the dynamical system evaluated in  $\bar{x}$ , and  $R_i = \sum_{j=1, j \neq i}^n |J_{ij}|$  for  $i = 1, \dots, n$ . If  $J_{ii} < 0$  and  $R_i < |J_{ii}|$  for  $i = 1, \dots, n$ , then  $\bar{x}$  is locally asymptotically stable.*

Using Theorem 3.3, the first condition  $J_{ii} < 0$  for  $i = 1, \dots, 6$  leads to

$$\alpha_1 < k_1M_c^* + \mu_1 + s_1, \quad \gamma_{aa}C^* < (1 - k_2)P_2^* + \mu_{aa}, \quad \alpha_2 < k_2M_{aa}^* + \mu_2, \quad \alpha_I C^* < \alpha_c + \alpha_{aa}P_2^* + \mu_n, \quad \gamma_c C^* < \mu_c.$$

The second condition,  $R_i < |J_{ii}|$  for  $i = 1, \dots, 6$  leads to

$$\begin{aligned} \frac{2|(1 - k_1)M_c^* - M_n^*\alpha_n| + \alpha_{p1}M_c^* + s_1}{L_0} < 1, & \quad \frac{\alpha_c + \alpha_{aa}P_2^* + \alpha_I C^*}{L_6} < 1, & \quad \frac{(1 - k_2)P_2^* + \alpha_{p2}P_2^* - \gamma_{aa}C^* + k_2P_2^*}{L_3} < 1, \\ \frac{\gamma_c C^*}{L_7} < 1, & \quad \frac{\alpha_I M_n^* + \gamma_c M_c^* + \gamma_{aa}M_{aa}^*}{\alpha_I M_n^* + \gamma_{aa}M_{aa}^* + \gamma_c M_c^* + \mu_s} < 1, & \quad \frac{2|(1 - k_2)M_{aa}^* - \alpha_{aa}M_n^*| + \alpha_{p2}M_{aa}^*}{L_5} < 1. \end{aligned}$$

The stability of the endemic point  $E_2^*$  depends on the stability of the Jacobian matrix  $J(E_2^*)$  given by

$$J(E_2^*) = \begin{pmatrix} L_0 & 0 & -k_1P_1^{**} & 0 & 0 & 0 \\ (1 - k_1)M_c^{**} - M_n^{**}\alpha_n & L_1 & (1 - k_1)P_1^{**} & (1 - k_2)P_2^{**} & \alpha_I M_n^{**} & (1 - k_2)M_{aa}^{**} - \alpha_{aa}M_n^{**} \\ M_n^{**}\alpha_n - (1 - k_1)M_c^{**} & \alpha_n P_1^{**} + \alpha_c & L_2 & 0 & \gamma_c M_c^{**} & 0 \\ 0 & \alpha_{aa}P_2^{**} & 0 & L_3 & \gamma_{aa}M_{aa}^{**} & \alpha_{aa}M_n^{**} - (1 - k_2)M_{aa}^{**} \\ \alpha_{p1}M_c^{**} & -\alpha_I C^{**} & \alpha_{p1}P_1^{**} - \gamma_c C^{**} & \alpha_{p2}P_2^{**} - \gamma_{aa}C^{**} & L_4 & \alpha_{p2}M_{aa}^{**} \\ s_1 & 0 & 0 & -k_2P_2^{**} & 0 & L_5 \end{pmatrix}$$

where

$$\begin{aligned} L_0 &= \alpha_1 - k_1M_c^{**} - \mu_1 - s_1, & L_1 &= \alpha_I C^{**} - \alpha_c P_1^{**} - \alpha_c - \alpha_{aa}P_2^{**} - \mu_n, & L_2 &= \gamma_c C^{**} - (1 - k_1)P_1^{**} - \mu_c, \\ L_3 &= \gamma_{aa}C^{**} - (1 - k_2)P_2^{**} - \mu_{aa}, & L_4 &= -\alpha_I M_n^{**} - \gamma_{aa}M_{aa}^{**} - \gamma_c M_c^{**} - \mu_s, & L_5 &= \alpha_2 - k_2M_{aa}^{**} - \mu_2. \end{aligned}$$

Similarly, applying Theorem 3.3 to  $J(E_2^*)$  with size  $6 \times 6$  we get the following inequalities:

$$\begin{aligned} \alpha_1 &< k_1M_c^{**} + \mu_1 + s_1, & \alpha_I C^{**} &< \alpha_c P_1^{**} + \alpha_c + \alpha_{aa}P_2^{**} + \mu_n, & \gamma_c C^{**} &< (1 - k_1)P_1^{**} + \mu_c, \\ \gamma_{aa}C^{**} &< (1 - k_2)P_2^{**} + \mu_{aa}, & \alpha_2 &< k_2M_{aa}^{**} + \mu_2. \end{aligned}$$

According to the Gershgorian theorem,  $R_i < |J_{ii}|$  for  $i = 1, \dots, 6$  is equivalent to  $R_j < |J_{jj}|$  for  $j = 1, \dots, 6$ . Using Theorem 3.3 on matrix  $J(E_2^*)$  with size  $6 \times 6$  we get the following inequalities:

$$\frac{2|(1 - k_1)M_c^{**} - M_n^{**} \alpha_n| + \alpha_{p1}M_c^{**} + s_1}{L_0} < 1, \quad \frac{\alpha_n P_1^{**} + \alpha_c + \alpha_{aa} P_2^{**} + \alpha_I C^{**}}{L_1} < 1, \tag{8}$$

$$\frac{(1 - k_1)P_1^{**} + |\alpha_{p1}P_1^{**} - \gamma_c C^{**}| + k_1 P_1^{**}}{L_2} < 1, \quad \frac{(1 - k_2)P_2^{**} + |\alpha_{p2}P_2^{**} - \gamma_{aa} C^{**}| + k_2 P_2^{**}}{L_3} < 1, \tag{9}$$

$$\frac{\alpha_I M_n^{**} + \gamma_c M_c^{**} + \gamma_{aa} M_{aa}^{**}}{\alpha_I M_n^{**} + \gamma_{aa} M_{aa}^{**} + \gamma_c M_c^{**} + \mu_s} < 1, \quad \frac{2|(1 - k_2)M_{aa}^{**} - \alpha_{aa} M_n^{**}| + \alpha_{p2} M_{aa}^{**}}{L_5} < 1. \tag{10}$$

Therefore, we conclude that the equilibrium point  $E_2^*$  is locally stable only provided the conditions given in Equation (8)–(10) hold.

## 4 Numerical Solutions

This section presents numerical simulations of the system of equations (1)–(6). The model simulations were carried out using the MATLAB software, using the parameter values in Table 3 and initial values in Table 2. Due to lack of information on the immunological dynamics for the sleeping sickness disease obtaining the parameter values presented some challenges. Few parameter values were obtained from published literature, while others were assumed based on assumptions made in the model formulation and in comparison with the dynamics of other tropical diseases like malaria, whose parasite exhibit similar characteristics as the HAT parasite (Mhlanga et al., 1997). Therefore our results are purely theoretical but qualitatively sound.

The model simulations gave us an insight into the effects of parasite switching on the evolution of HAT and how the disease progresses over time in the human host. In order to investigate the effects of parasite switching, we first simulate the model when the switch parameter is zero. Figures 2–4 illustrate the evolution of various populations in this scenario. From Figures 2 and 3, it can be seen that with no switching of the parasite, the innate immune response is adequate to deal with the pathogen. The parasite is cleared within a week of infection. During that same period, there is a rise in the levels of naive and classical macrophages (Figure 3) as well as cytokines levels (Figure 4) in the host. It can be noted that the levels of macrophages and cytokines decrease after the pathogen has been dealt with. This highlights the significant role played by both macrophages and cytokines in the innate immune response, immediately after infection, to limit the spread of the pathogen. Moreover, it can be noted that when the innate response is effective against the infection, adaptive response is not required.

In the second scenario, we allow the parasite to switch to another parasite type. The response of various populations to the switch is shown in Figures 5–8, when the value of the switching parameter is  $s_1 = 0.0001$ . The way at which the parasite evades the immune response by switching type to different parasite type, can be depicted in Figure 5. This is illustrated by exponential rise of the type 2 parasite, two weeks after infection. Figure 7 show cases the host adaptive immune response to the resurgent parasite, characterise by the activation of alternative activated macrophages, whose role is to deal with the new rise in the type 2 pathogen. Figure 8 show cases the cytokine concentration which justifies the behaviour of alternative activated macrophages.

## 5 Optimal Control Strategies

In this section, we formulate two optimal control models by modifying the system of equations (1)–(6), to incorporate the effect of different drug strategies. Often the treatment of HAT patients depends on the stage of the disease at which the patient is diagnosed. Drugs can be categorized into two types:

- Initial stage drug and
- Second stage drug.

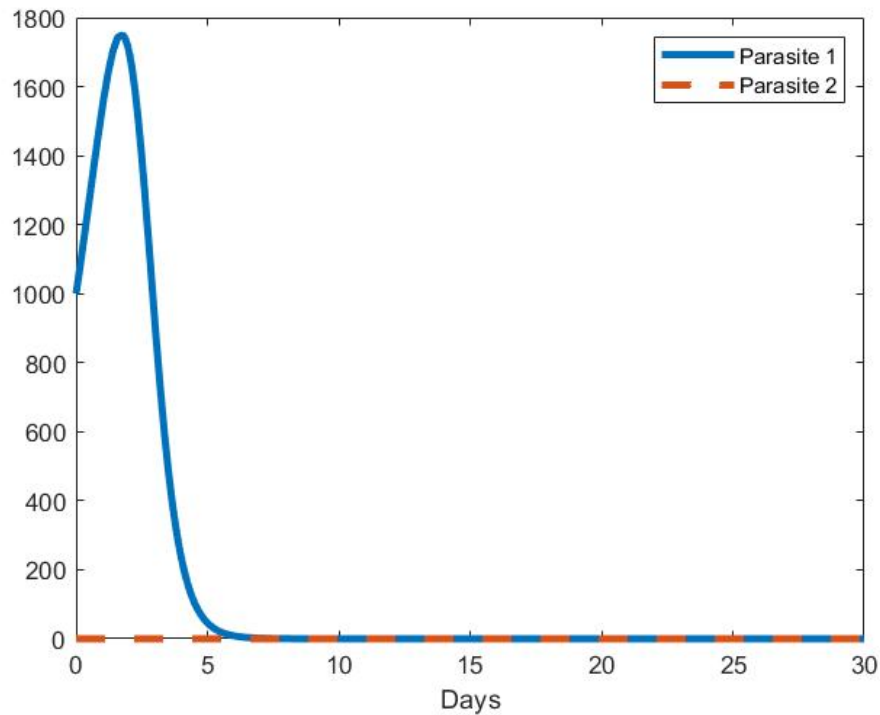
### 5.1 Initial stage drug

These are drugs that are administered in the early stage of the disease, due to their inability to cross the blood brain barrier. This for instance is the case of Pentamidine, Suramin (Etcheberry et al., 2001). The main function of these drugs is to reduce the parasite load in the host. Our performance measure is to minimize the parasites load in a finite time  $t_f$ . The corresponding optimal control problem is

$$\text{minimise} \{J = P_1(t_f) + P_2(t_f)\}.$$

**Table 3:** Parameter values.

Parameter	Value	Units	References
$\alpha_1$	0.75	day <sup>-1</sup>	Wockner et al., 2020
$s_1$	0.0001	day <sup>-1</sup>	Frank, 1999
$k_1$	0.00045	day <sup>-1</sup>	Assumed
$\mu_1$	0.45	day <sup>-1</sup>	Assumed
$\Lambda_n$	100	cells/ml/day <sup>-1</sup>	Assumed
$\alpha_n$	0.5	day <sup>-1</sup>	Assumed
$\alpha_c$	0.00304	day <sup>-1</sup>	Assumed
$\alpha_{aa}$	0.0045	day <sup>-1</sup>	Assumed
$\alpha_I$	0.4	day <sup>-1</sup>	Mohamed et al., 2018
$\mu_n$	0.02	day <sup>-1</sup>	Pienaar and Lerm, 2014
$\gamma_c$	0.4	day <sup>-1</sup>	Mohamed et al., 2018
$\mu_c$	0.02	day <sup>-1</sup>	Pienaar and Lerm, 2014
$\gamma_{aa}$	0.4	day <sup>-1</sup>	Assumed
$\mu_s$	0.0154	day <sup>-1</sup>	Assumed
$\alpha_{p1}$	0.0015	day <sup>-1</sup>	Assumed
$\alpha_{p2}$	0.006	day <sup>-1</sup>	Assumed
$k_2$	0.0006	day <sup>-1</sup>	Assumed
$\mu_{aa}$	0.02	day <sup>-1</sup>	Pienaar and Lerm, 2014
$\alpha_2$	0.8	day <sup>-1</sup>	Assumed
$\mu_2$	0.45	day <sup>-1</sup>	Assumed
$d_0$	0.2	day <sup>-1</sup>	Assumed
$d_1$	0.02	day <sup>-1</sup>	Assumed
$\mu_u$	0.00045	day <sup>-1</sup>	Assumed

**Figure 2:** Numerical solution showing progression of the parasite types with no parasite switching.

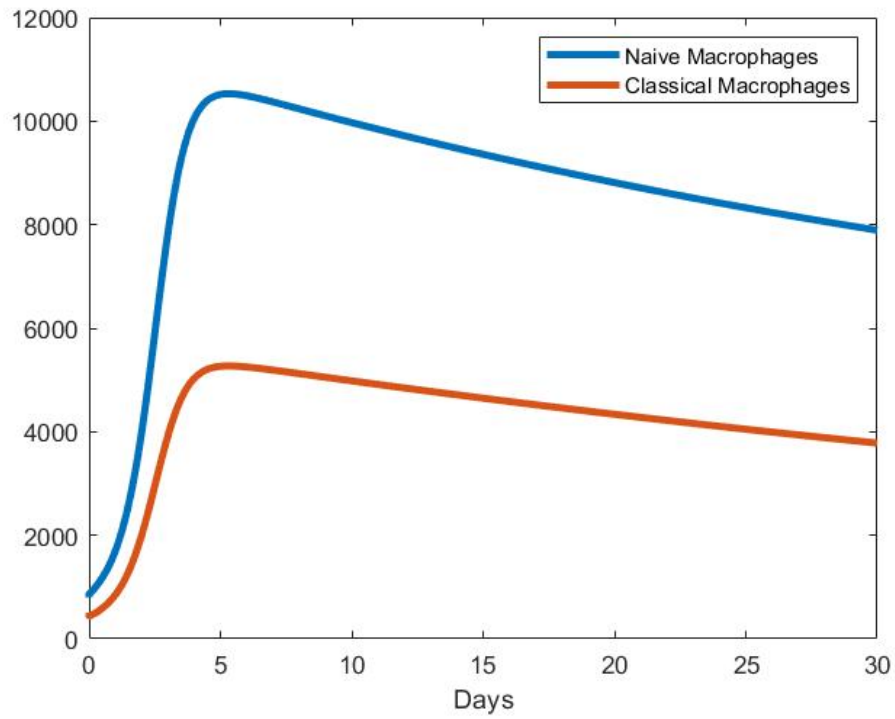


Figure 3: Numerical solution showing progression of the naive and classical macrophages with no parasite switching.

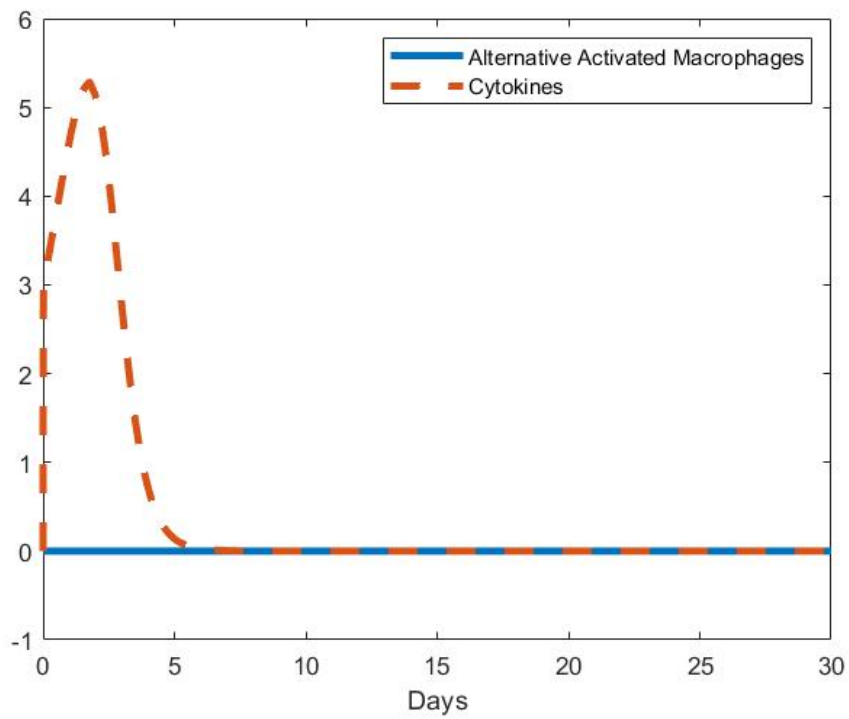
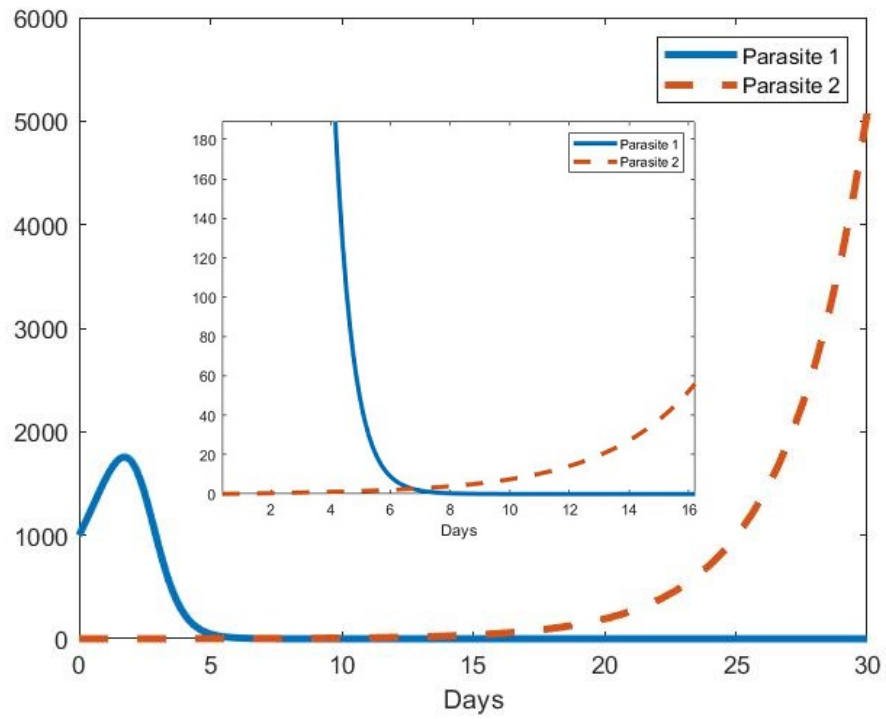
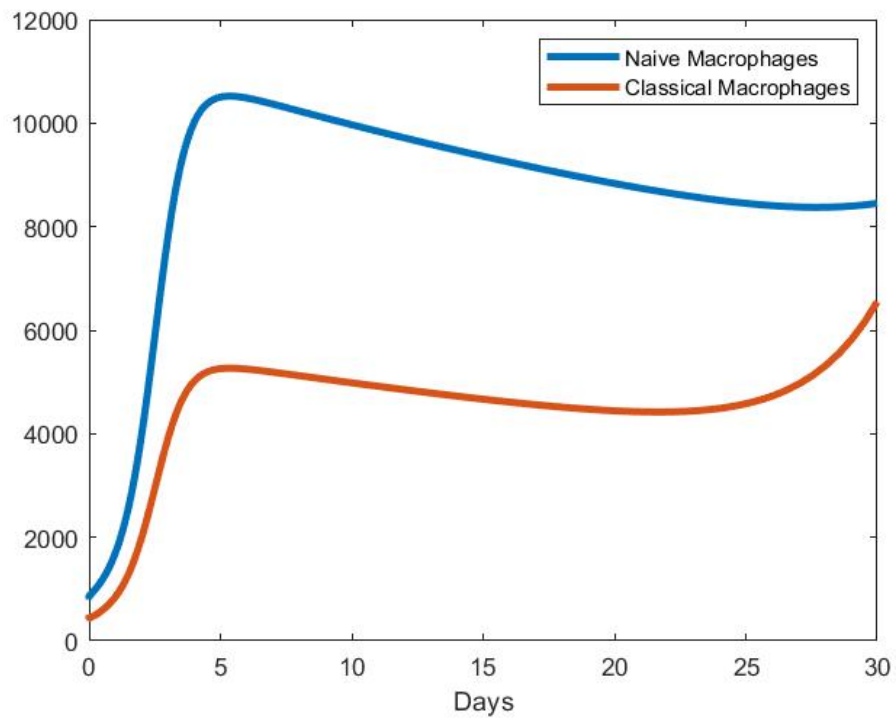


Figure 4: Numerical solution showing progression of the alternative activated macrophages and the cytokines levels with no parasite switching.



**Figure 5:** Numerical solution showing progression of the parasite types with parasite switching.



**Figure 6:** Numerical solution showing progression of the naive and classical macrophages with parasite switching.

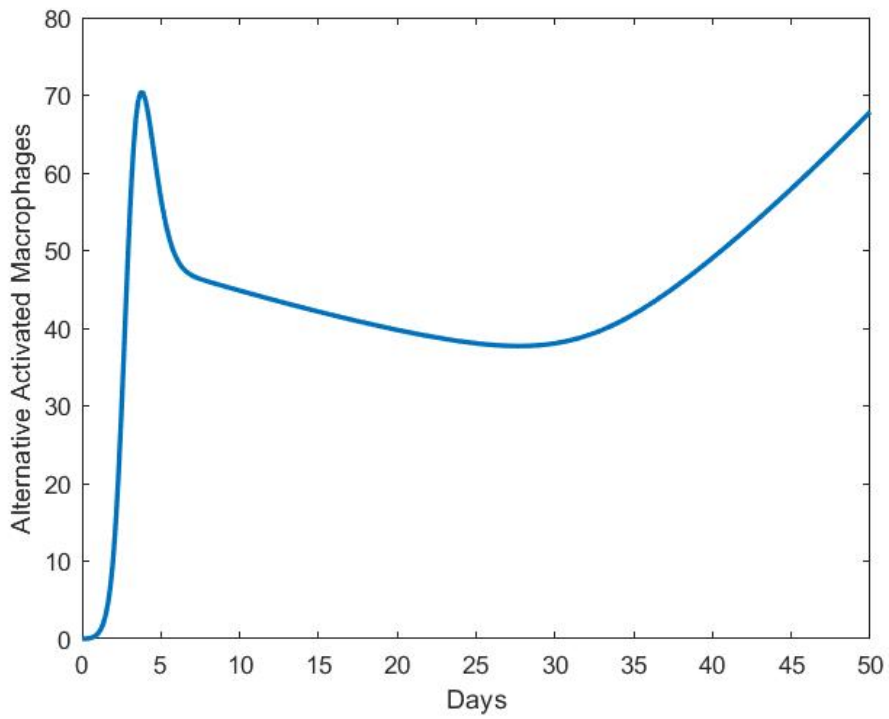


**Figure 7:** Numerical solution showing progression of the alternative activated macrophages with parasite switching.

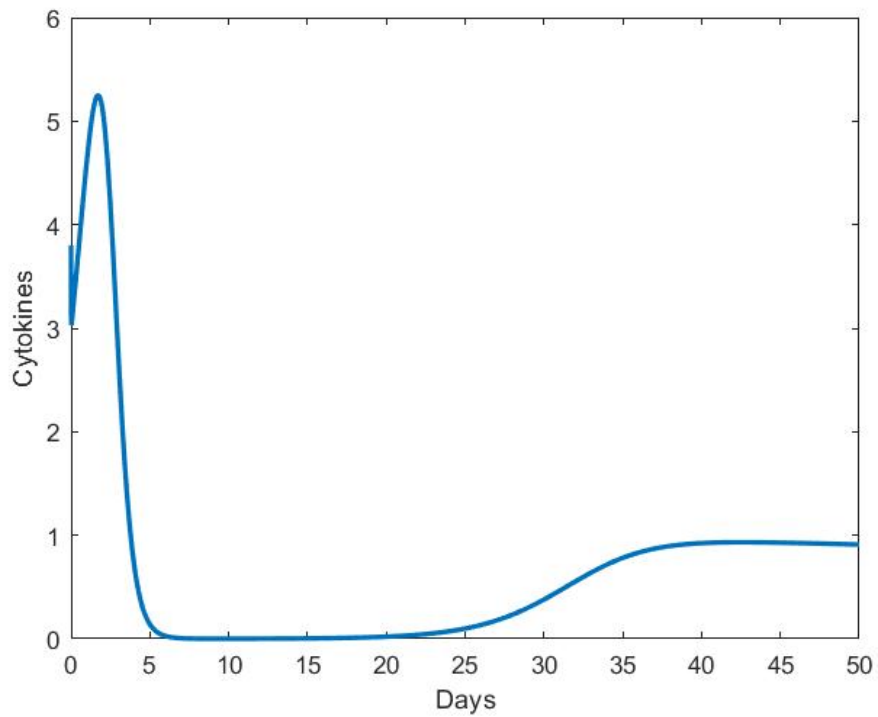


**Figure 8:** Numerical solution showing progression of the cytokine concentration with parasite switching.

subject to

$$\left\{ \begin{array}{l} \frac{dP_1}{dt} = \alpha_1 P_1 - d_0(1 - e^{-U})P_1 - s_1 P_1 - k_1 P_1 M_c - \mu_1 P_1, \quad P_1(0) = P_1^0; \\ \frac{dM_n}{dt} = \Lambda_n - \alpha_n M_n P_1 + (1 - k_1)P_1 M_c + (1 - k_2)P_2 M_{aa} - \alpha_c M_n - \alpha_{aa} M_n P_2 + \alpha_I M_n C \\ \quad - \mu_n M_n - d_1(1 - e^{-U})M_n, \quad M_n(0) = M_n^0; \\ \frac{dM_c}{dt} = \alpha_n M_n P_1 + \alpha_c M_n + \gamma_c M_c C - (1 - k_1)P_1 M_c - \mu_c M_c - d_1(1 - e^{-U})M_c, \quad M_c(0) = M_c^0; \\ \frac{dM_{aa}}{dt} = \alpha_{aa} M_n P_2 + \gamma_{aa} M_{aa} C - (1 - k_2)P_2 M_{aa} - \mu_{aa} M_{aa} - d_1(1 - e^{-U})M_{aa}, \quad M_{aa}(0) = M_{aa}^0; \\ \frac{dC}{dt} = \alpha_{p1} P_1 M_c + \alpha_{p2} P_2 M_{aa} - \alpha_I M_n C - \gamma_{aa} M_{aa} C - \gamma_c M_c C - \mu_s C, \quad C(0) = C^0; \\ \frac{dP_2}{dt} = s_1 P_1 + \alpha_2 P_2 - d_0(1 - e^{-U})P_2 - k_2 P_2 M_{aa} - \mu_2 P_2, \quad P_2(0) = P_2^0; \\ \frac{dU}{dt} = v(t) - \mu_u U, \quad U(0) = U^0 \end{array} \right. \quad (11)$$

where  $P_1^0, M_n^0, M_c^0, M_{aa}^0, C^0, P_2^0, U^0$  are positive constants at  $0 \leq v(t) \leq v_{\max}$ , with  $v_{\max}$  being the maximum dosage possible.

In the model system (11), we denote the amount of drug in the human host at time  $t$  by  $U(t)$ . The drug kills the parasite, and we assume that the drug is toxic to the immune cells. This is represented by the fraction kill for an amount of drug introduced to the system (De Pellis and Radunskaya, 2000). The fraction kill is given by

$$z(U) = d_i(1 - e^{-kU}) \quad \text{for } i = 1, 2.$$

Certain aspects in the pharmacokinetics are still unrevealed in this current study, we let  $k = 1$ . We let  $d_1$  denote the parasite drug response coefficient, with  $d_0$  being the cell drug response coefficient with an assumption that  $d_0 > d_1$ . The amount of drug in the host is determined by the drug dosage  $v(t)$  given at a particular time. It is assumed that the drug decays naturally at a rate  $\mu_u$ . It is important to note that the control is not effective when  $U = 0$  and effective when  $U \neq 0$ .

**Theorem 5.1.** *Given the optimal control variable  $v(t)$ , and corresponding state variables  $P_1, M_n, M_c, M_{aa}, C$ , and  $P_2$  of the control system (11), and initial conditions in Table 2 admit a unique optimal solution  $P_1^*, M_n^*, M_c^*, M_{aa}^*, C^*, P_2^*$  associated with an optimal control  $v(t)$  with a fixed optimal final time  $t_f$ ; moreover, there exists adjoint co-state functions  $\lambda_i(t), 1 \leq i \leq 7$ , satisfying  $\frac{d\lambda_1}{dt} = -\frac{\partial H}{\partial P_1}, \frac{d\lambda_2}{dt} = -\frac{\partial H}{\partial M_n}, \frac{d\lambda_3}{dt} = -\frac{\partial H}{\partial M_c}, \frac{d\lambda_4}{dt} = -\frac{\partial H}{\partial M_{aa}}, \frac{d\lambda_5}{dt} = -\frac{\partial H}{\partial C}, \frac{d\lambda_6}{dt} = -\frac{\partial H}{\partial P_2}, \frac{d\lambda_7}{dt} = -\frac{\partial H}{\partial U}$  with corresponding transversality conditions  $\lambda_1(t_f) = 1, \lambda_2(t_f) = 0, \lambda_3(t_f) = 0, \lambda_4(t_f) = 0, \lambda_5(t_f) = 0, \lambda_6(t_f) = 1$ , and  $\lambda_7(t_f) = 0$ . The Hamiltonian function  $H$  for the optimal control problem is given by*

$$H = J + \lambda_1 \dot{P}_1 + \lambda_2 \dot{M}_n + \lambda_3 \dot{M}_c + \lambda_4 \dot{M}_{aa} + \lambda_5 \dot{C} + \lambda_6 \dot{P}_2 + \lambda_7 \dot{U}$$

Furthermore, the optimal control dosage is given by

$$v(t) = \begin{cases} 0, & \text{if } \lambda_7 > 0, \\ v_{\max}, & \text{if } \lambda_7 < 0, \\ \text{undetermined,} & \text{if } \lambda_7 = 0. \end{cases}$$

*Proof.* According to Pontryagin maximum principle (Pontryagin et al., 1986), we have the Hamiltonian function defined as,

$$\begin{aligned} H = & A_1 P_1 + A_2 P_2 + \lambda_1 [\alpha_1 P_1 - d_0(1 - e^{-U})P_1 - s_1 P_1 - k_1 P_1 M_c - \mu_1 P_1] \\ & + \lambda_2 [\Lambda_n - \alpha_n M_n P_1 + (1 - k_1)P_1 M_c + (1 - k_2)P_2 M_{aa} - \alpha_c M_n - \alpha_{aa} M_n P_2 + \alpha_I M_n C - \mu_n M_n - d_1(1 - e^{-U})M_n] \\ & + \lambda_3 [\alpha_n M_n P_1 + \alpha_c M_n + \gamma_c M_c C - (1 - k_1)P_1 M_c - \mu_c M_c - d_1(1 - e^{-U})M_c] \\ & + \lambda_4 [\alpha_{aa} M_n P_2 + \gamma_{aa} M_{aa} C - (1 - k_2)P_2 M_{aa} - \mu_{aa} M_{aa} - d_1(1 - e^{-U})M_{aa}] \\ & + \lambda_5 [\alpha_{p1} P_1 M_c + \alpha_{p2} P_2 M_{aa} - \alpha_I M_n C - \gamma_{aa} M_{aa} C - \gamma_c M_c C - \mu_s C] \\ & + \lambda_6 [s_1 P_1 + \alpha_2 P_2 - d_0(1 - e^{-U})P_2 - k_2 P_2 M_{aa} - \mu_2 P_2] \\ & + \lambda_7 [v(t) - \mu_u U], \end{aligned}$$

where  $\lambda_1, \lambda_2, \lambda_3, \lambda_4, \lambda_5, \lambda_6,$  and  $\lambda_7$  are the adjoint functions associated with the state functions. Applying the Pontryagin maximum principle, the adjoint system is given by

$$\begin{aligned} \frac{d\lambda_1}{dt} &= -A_1 + \lambda_1[d_0(1 - e^{-U}) + s_1 + k_1M_c - \mu_1 - \alpha_1] + \alpha_2M_n\lambda_2 + \lambda_3[(1 - k_1)M_c - \alpha_nM_n] - \lambda_6s_1 - \lambda_5\alpha_{p1}M_c \\ \frac{d\lambda_2}{dt} &= \lambda_2[\alpha_nP_1 + \alpha_c - \alpha_I C + \alpha_{aa}P_2 + \mu_n + d_1(1 - e^{-U})] + \lambda_5\alpha_I C - \lambda_4\alpha_{aa}P_2 - \lambda_3[\alpha_nP_1 + \alpha_c] \\ \frac{d\lambda_3}{dt} &= \lambda_1k_1P_1 - \lambda_2(1 - k_1)P_1 + \lambda_3[(1 - k_1)P_1 + \mu_c + d_1(1 - e^{-U}) - \gamma_c C] + \lambda_5[\gamma_c C - \alpha_{p1}P_1] \\ \frac{d\lambda_4}{dt} &= \lambda_6k_2P_2 - \lambda_2(1 - k_2)P_2 + \lambda_4[(1 - k_2)P_2 + \mu_{aa} + d_1(1 - e^{-U}) - \gamma_{aa} C] + \lambda_5[\gamma_{aa} C - \alpha_{p2}P_2] \\ \frac{d\lambda_5}{dt} &= \lambda_5[\alpha_I M_n + \gamma_{aa}M_{aa} + \gamma_c M_c + \mu_s] - \lambda_2\alpha_I M_n - \lambda_3\gamma_c M_c - \lambda_4\gamma_{aa}M_{aa} \\ \frac{d\lambda_6}{dt} &= -A_2 + \lambda_2[\alpha_{aa}M_n - (1 - k_2)M_{aa}] + \lambda_4[(1 - k_2)M_{aa} - \alpha_{aa}M_n] - \lambda_5\alpha_{p2}M_{aa} \\ &\quad + \lambda_6[k_2M_{aa} + d_0(1 - e^{-U}) + \mu_2 - \alpha_2] \\ \frac{d\lambda_7}{dt} &= e^{-U}(\lambda_1d_0P_1 + \lambda_2d_1M_n + \lambda_3d_1M_c + \lambda_4d_1M_{aa} + \lambda_6d_0P_2) + \lambda_7\mu_u. \end{aligned}$$

Using the transversality condition, the initial values for the adjoint functions are obtained as

$$\begin{aligned} \lambda_1(t_f) = \frac{\partial J}{\partial P_1} \Big|_{t=t_f} &= 1, & \lambda_2(t_f) = \frac{\partial J}{\partial M_n} \Big|_{t=t_f} &= 0, & \lambda_3(t_f) = \frac{\partial J}{\partial M_c} \Big|_{t=t_f} &= 0, & \lambda_4(t_f) = \frac{\partial J}{\partial M_{aa}} \Big|_{t=t_f} &= 0, \\ \lambda_5(t_f) = \frac{\partial J}{\partial C} \Big|_{t=t_f} &= 0, & \lambda_6(t_f) = \frac{\partial J}{\partial P_2} \Big|_{t=t_f} &= 1, & \lambda_7(t_f) = \frac{\partial J}{\partial U} \Big|_{t=t_f} &= 0. \end{aligned}$$

The drug in the whole system is dependent on the dosage given at a particular time. The aim is to minimise the Hamiltonian  $H$ , with respect to the dosage  $v$ . But  $H$  is linear in  $v$

$$H = \lambda_7v + \lambda_8,$$

where  $\lambda_8 = A_1P_1 + A_2P_2 + \lambda_1\dot{P}_1 + \lambda_2\dot{M}_n + \lambda_3\dot{M}_c + \lambda_4\dot{M}_{aa} + \lambda_5\dot{C} + \lambda_6\dot{P}_2 - \mu_u\lambda_7\dot{U}$ . Thus the optimal value  $v(t)$

$$v(t) = \begin{cases} 0, & \text{if } \lambda_7 > 0, \\ v_{max}, & \text{if } \lambda_7 < 0, \\ \text{undetermined,} & \text{if } \lambda_7 = 0. \end{cases}$$

The adjoint function  $\lambda_7$  is the switching function for the drug dosage  $v(t)$ , bounded by  $0 \leq v(t) \leq v_{max}$ ; the drug should be injected at maximum rate,  $v_{max}$ , whenever  $\lambda_7$  is negative and should be stopped whenever  $\lambda_7$  is positive.  $\square$

### 5.1.1 Numerical simulations of early stage stage drug

We use the steepest descent method to find the optimal control, in combination with the forward, backward sweep method for the state and co-state variables. We note that the drug dosage needs to be the same every day. The initial conditions for model (11) are given by  $P_1 = 1000, M_n = 500, M_c = 300, M_{aa} = 10, C = 5, P_2 = 500$ , with the assumption that intervention is implemented when the disease has progressed in the human host. The solution curve (blue) without intervention was simulated with the initial conditions in Table 2. From Figure 9, we notice the significant reduction of the parasite type 1 population in the presence of the drug as opposed to no drug in the system. From Figure 12, we notice that in spite of the drug being present in the system, parasite type 2 increases with time. This suggests that using a drug targeting the parasite population does not reduce the disease burden. We observe a decline in the macrophage populations in Figures 10, 11, and 14 when using the first stage drug. That is because the drug has a negative impact on macrophages because of the toxicity of the drug. This then means that the body loses its ability to fight parasites. Attributes shown in Figure 12 confirms that not any drug minimises the disease burden in the system. Figure 15 illustrates that early stage drugs need to be administered continuously for 10 days.

## 5.2 Second stage drug

In the second optimal control strategy, the specific function of the drug is to reduce the parasite load by targeting their production abilities. These are drugs that are administered in the second stage of the disease, due to their ability to cross the blood brain

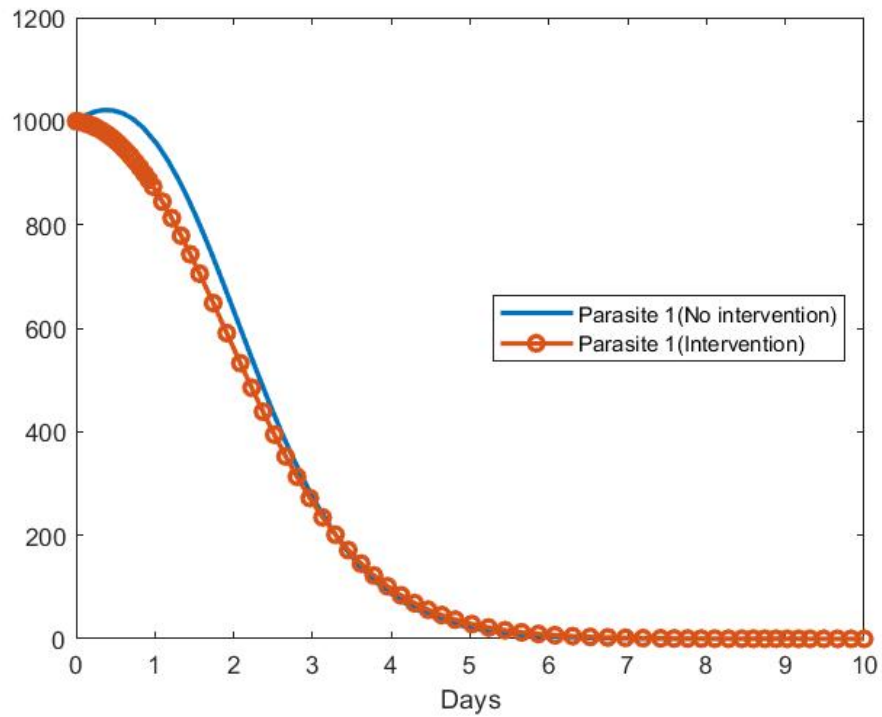


**Figure 9:** Numerical solutions of model system showing progression of parasite type 1 with effects of the early stage drug.

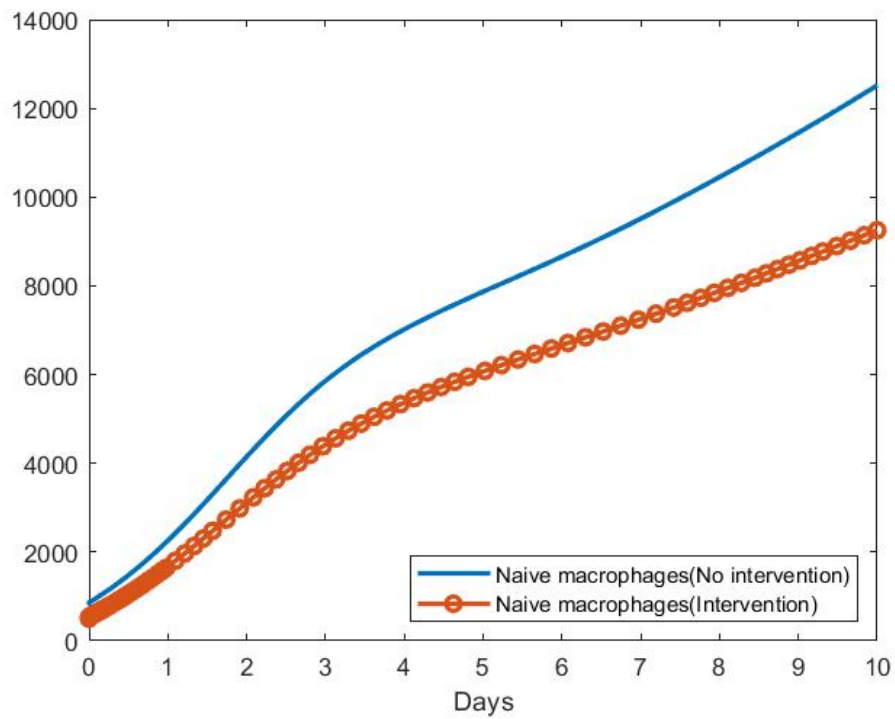


**Figure 10:** Numerical solutions of model system showing progression of naive macrophages with effects of the early stage drug.

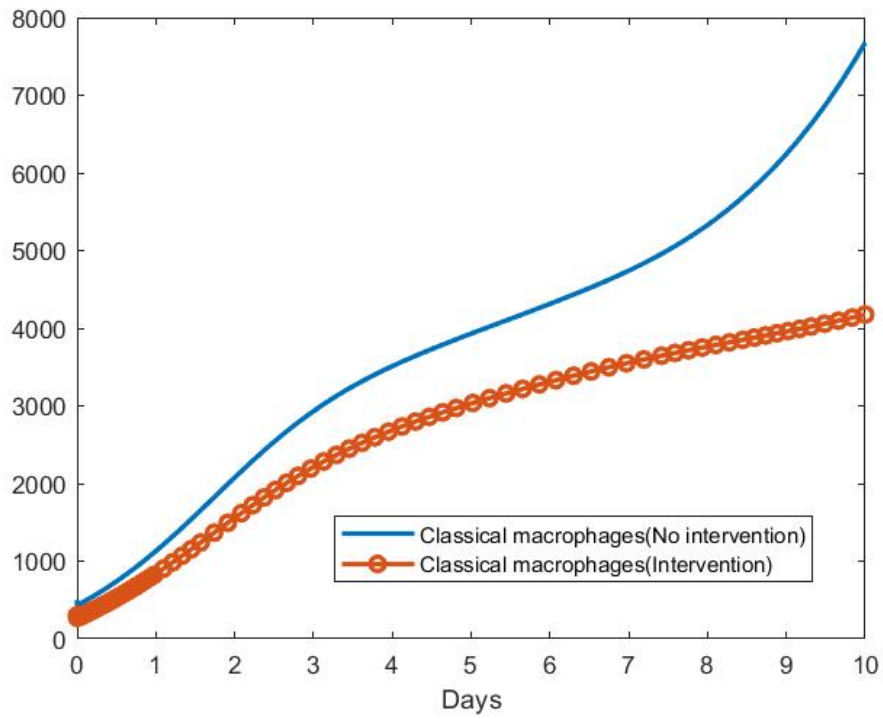


**Figure 11:** Numerical solutions of model system showing progression of classical macrophages with effects of the early stage drug.

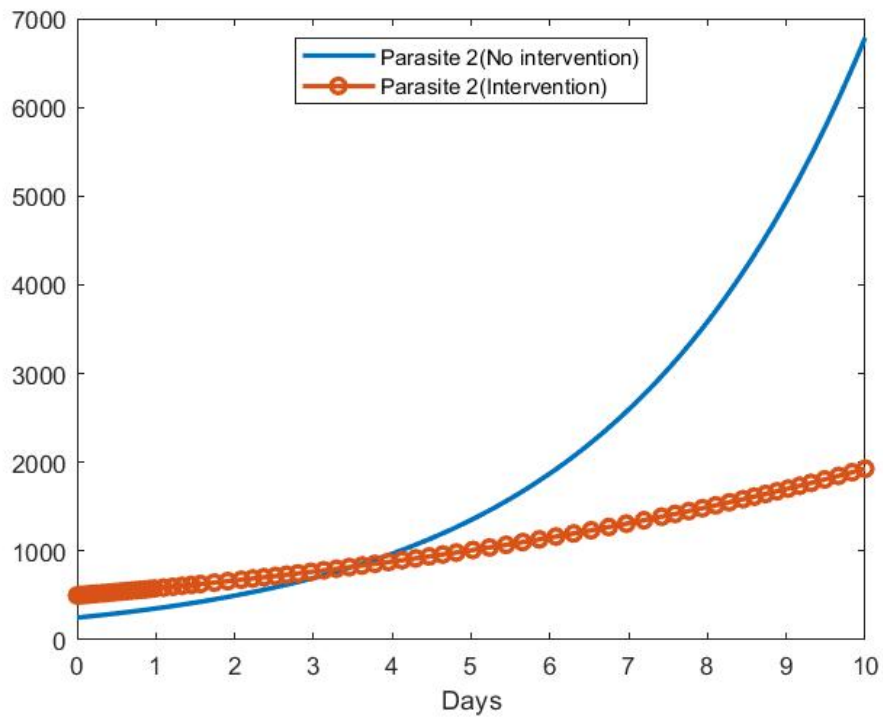


**Figure 12:** Numerical solutions of model system showing progression of parasite type 2 with effects of the early stage drug

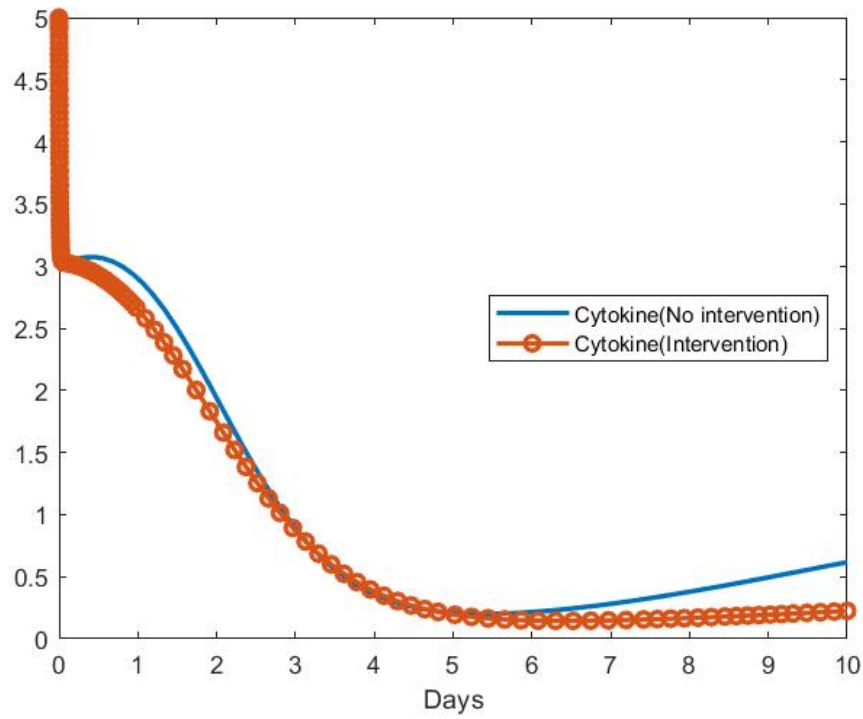


**Figure 13:** Numerical solutions of model system showing progression of cytokines with effects of the early stage drug.

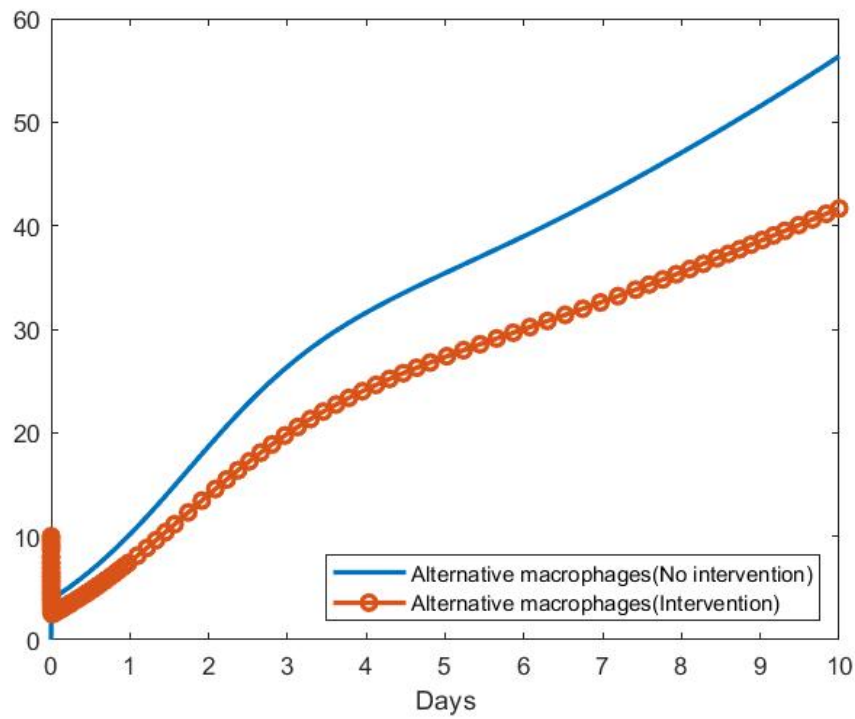


**Figure 14:** Numerical solutions of model system showing progression of alternative macrophages with effects of the early stage drug.

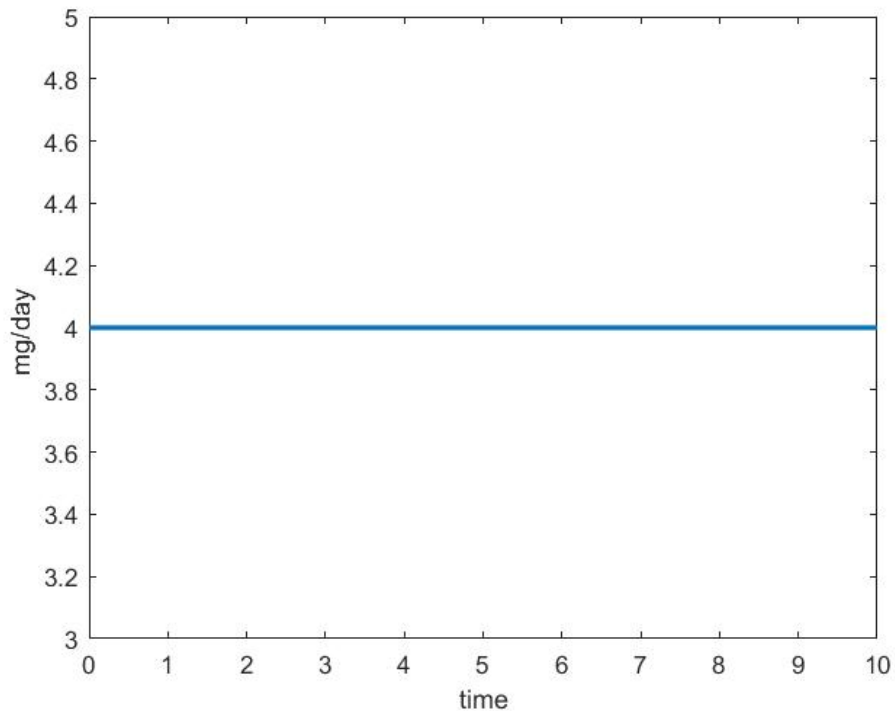


**Figure 15:** Drug dosage

barrier. This for instance is the case of Melarsoprol, Eflornithine, and Fexinidazole (Etchegorry et al., 2001). In this strategy, the performance measure is given by

$$J = \int_{t_0}^{t_f} (A_1 P_1 + A_2 P_2 + b_2 u_2^2 - b_1 u_1^2) dt.$$

Thus, we wish to minimise the density of parasite  $P_1, P_2$  and the toxicity of the drug  $u_2$ , while maximising drug efficacy. The corresponding optimal control problem is

$$\text{minimise} \left\{ J = \int_{t_0}^{t_f} (A_1 P_1 + A_2 P_2 + b_2 u_2^2 - b_1 u_1^2) dt \right\}.$$

subject to

$$\left\{ \begin{array}{l} \frac{dP_1}{dt} = (1 - u_1)\alpha_1 P_1 - s_1 P_1 - k_1 P_1 M_c - \mu_1 P_1, \quad P_1(0) = P_1^0; \\ \frac{dM_n}{dt} = \Lambda_n - \alpha_n M_n P_1 + (1 - k_1) P_1 M_c + (1 - k_2) P_2 M_{aa} \\ \quad - \alpha_c M_n - \alpha_{aa} M_n P_2 + \alpha_I M_n C - (\mu_n + u_2) M_n, \quad M_n(0) = M_n^0; \\ \frac{dM_c}{dt} = \alpha_n M_n P_1 + \alpha_c M_n + \gamma_c M_c C - (1 - k_1) P_1 M_c - (\mu_c + u_2) M_c, \quad M_c(0) = M_c^0; \\ \frac{dM_{aa}}{dt} = \alpha_{aa} M_n P_2 + \gamma_{aa} M_{aa} C - (1 - k_2) P_2 M_{aa} - (\mu_{aa} + u_2) M_{aa}, \quad M_{aa}(0) = M_{aa}^0; \\ \frac{dC}{dt} = \alpha_{p1} P_1 M_c + \alpha_{p2} P_2 M_{aa} - \alpha_I M_n C - \gamma_{aa} M_{aa} C - \gamma_c M_c C - \mu_s C, \quad C(0) = C^0; \\ \frac{dP_2}{dt} = s_1 P_1 + (1 - u_1)\alpha_2 P_2 - k_2 P_2 M_{aa} - \mu_2 P_2, \quad P_2(0) = P_2^0 \end{array} \right. \quad (12)$$

where  $P_1^0, M_n^0, M_c^0, M_{aa}^0, C^0, P_2^0$  are given constants and  $0 \leq u_1(t) \leq 1; u_2(t) \geq 0$  with  $u_1 = 1$  being 100% effective and  $u_1 = 0$  being no drug usage.

**Theorem 5.2.** *Given the optimal control variable  $u_1, u_2$ , and corresponding state variables  $P_1, M_n, M_c, M_{aa}, C$ , and  $P_2$  of the control system (12), and initial conditions in Table 2 admits a unique optimal solution  $P_1^*, M_n^*, M_c^*, M_{aa}^*, C^*, P_2^*$  associated with an optimal control  $u_1, u_2$  with a fixed optimal final time  $t_f$ ; moreover, there exists adjoint co-state functions  $\lambda_i(t), 1 \leq i \leq 6$ , satisfying  $\frac{d\lambda_1}{dt} = -\frac{\partial H}{\partial P_1}, \frac{d\lambda_2}{dt} = -\frac{\partial H}{\partial M_n}, \frac{d\lambda_3}{dt} = -\frac{\partial H}{\partial M_c}, \frac{d\lambda_4}{dt} = -\frac{\partial H}{\partial M_{aa}}, \frac{d\lambda_5}{dt} = -\frac{\partial H}{\partial C}, \frac{d\lambda_6}{dt} = -\frac{\partial H}{\partial P_2}, \frac{d\lambda_7}{dt} = -\frac{\partial H}{\partial U}$ . The Hamiltonian function  $H$  for the optimal control problem is given by*

$$H = J + \lambda_1 \dot{P}_1 + \lambda_2 \dot{M}_n + \lambda_3 \dot{M}_c + \lambda_4 \dot{M}_{aa} + \lambda_5 \dot{C} + \lambda_6 \dot{P}_2.$$

Furthermore, the optimal control variable solutions are given as

$$u_1^* = \min \left\{ \max \left\{ 0, -\frac{1}{2b_1} (\lambda_1 \alpha_1 P_1 + \lambda_6 \alpha_2 P_2) \right\}, 1 \right\}.$$

*Proof.* According to the Pontryagin maximum principle (Pontryagin et al., 1986), the Hamiltonian function is defined by

$$\begin{aligned} H = & A_1 P_1 + A_2 P_2 + b_2 u_2^2 - b_1 u_1^2 + \lambda_1 [(1 - u_1) \alpha_1 P_1 - s_1 P_1 - k_1 P_1 M_c - \mu_1 P_1] \\ & + \lambda_2 [\Lambda_n - \alpha_n M_n P_1 + (1 - k_1) P_1 M_c + (1 - k_2) P_2 M_{aa} - \alpha_c M_n - \alpha_{aa} M_n P_2 + \alpha_I M_n C - (\mu_n + u_2) M_n] \\ & + \lambda_3 [\alpha_n M_n P_1 + \alpha_c M_n + \gamma_c M_c C - (1 - k_1) P_1 M_c - (\mu_c + u_2) M_c] \\ & + \lambda_4 [\alpha_{aa} P_2 M_n + \gamma_{aa} M_{aa} C - (1 - k_2) P_2 M_{aa} - (\mu_{aa} + u_2) M_{aa}] \\ & + \lambda_5 [\alpha_{p1} M_c P_1 + \alpha_{p2} P_2 M_{aa} - \alpha_I M_n C - \gamma_{aa} M_{aa} C - \gamma_c M_c C - \mu_s C] \\ & + \lambda_6 [s_1 P_1 + (1 - u_1) \alpha_2 P_2 - k_2 P_2 M_{aa} - \mu_2 P_2], \end{aligned}$$

where  $\lambda_1, \lambda_2, \lambda_3, \lambda_4, \lambda_5, \lambda_6$  are adjoint functions of the following adjoint system:

$$\begin{aligned} \frac{d\lambda_1}{dt} &= -A_1 + \lambda_1 [s_1 + k_1 M_c + \mu_1 - (1 - u_1) \alpha_1] + \lambda_2 [\alpha_n M_n - (1 - k_1) M_c] + \lambda_3 [(1 - k_1) M_c - \alpha_n M_n] - \lambda_5 \alpha_{p1} M_c - \lambda_6 s_1, \\ \frac{d\lambda_2}{dt} &= \lambda_2 [\alpha_n P_1 + \alpha_c + \alpha_{aa} P_2 + (\mu_n + u_2) - \alpha_I C] - \lambda_3 [\alpha_n P_1 + \alpha_c] - \lambda_4 \alpha_{aa} P_2 + \lambda_5 \alpha_I C, \\ \frac{d\lambda_3}{dt} &= \lambda_1 k_1 P_1 - \lambda_2 (1 - k_1) P_1 + \lambda_3 [(1 - k_1) P_1 + (\mu_c + u_2) - \gamma_c C] + \lambda_5 [\gamma_c C - \alpha_{p1} P_1], \\ \frac{d\lambda_4}{dt} &= k_2 P_2 \lambda_6 - \lambda_2 (1 - k_2) P_2 + \lambda_4 [(1 - k_2) P_2 + (\mu_{aa} + u_2) - \gamma_{aa} C] + \lambda_5 [\gamma_{aa} C - \alpha_{p2} P_2], \\ \frac{d\lambda_5}{dt} &= \lambda_5 (\alpha_I M_n + \gamma_{aa} M_{aa} + \gamma_c M_c + \mu_s) - \lambda_2 \alpha_I M_n - \lambda_3 \gamma_c M_c - \lambda_4 \gamma_{aa} M_{aa}, \\ \frac{d\lambda_6}{dt} &= -A_2 + \lambda_2 [\alpha_{aa} M_n - (1 - k_2) M_{aa}] + \lambda_4 [(1 - k_2) M_{aa} - \alpha_{aa} M_n] - \lambda_5 \alpha_{p2} M_{aa} + \lambda_6 [k_2 M_{aa} + \mu_2 - \alpha_2 (1 - u_1)]. \end{aligned}$$

Using the first derivative test, the optimal controls are obtained by solving

$$\frac{\partial H}{\partial u_1} = -2b_1 u_1 - \lambda_1 \alpha_1 P_1 - \lambda_6 \alpha_2 P_2 = 0, \tag{13}$$

$$\frac{\partial H}{\partial u_2} = 2b_2 u_2 - M_n \lambda_2 - M_c \lambda_3 - M_{aa} \lambda_4 = 0. \tag{14}$$

Solving for  $u_1$  and  $u_2$  in the system (13)–(14), the corresponding optimal control variable solutions are given by

$$\begin{aligned} u_1^* &= -\frac{1}{2b_1} (\lambda_1 \alpha_1 P_1 + \lambda_6 \alpha_2 P_2), \\ u_2^* &= \frac{1}{2b_2} (\lambda_2 M_n + M_c \lambda_3 + M_{aa} \lambda_4). \end{aligned} \quad \square$$

### 5.2.1 Numerical simulations of second stage drug

Similarly, we use the steepest descent method to find the optimal control, in combination with the forward, backward sweep method for the state and co-state variables.

Figures 16–21 illustrate the dynamics of model (12). Model (12) incorporates the drug that targets the growth rate of the parasite. In Figure 16, we notice that parasite type one ideally reduces in the presence of the drug. In Figure 19, we observe that

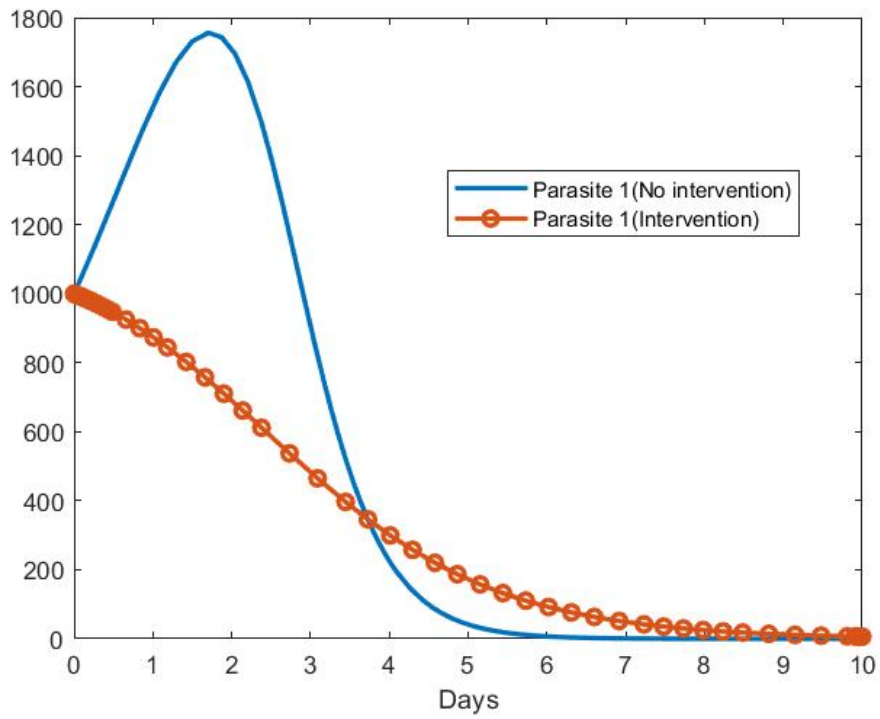


Figure 16: Numerical solutions of model system showing progression of parasite type 1 with effects of second stage drug.

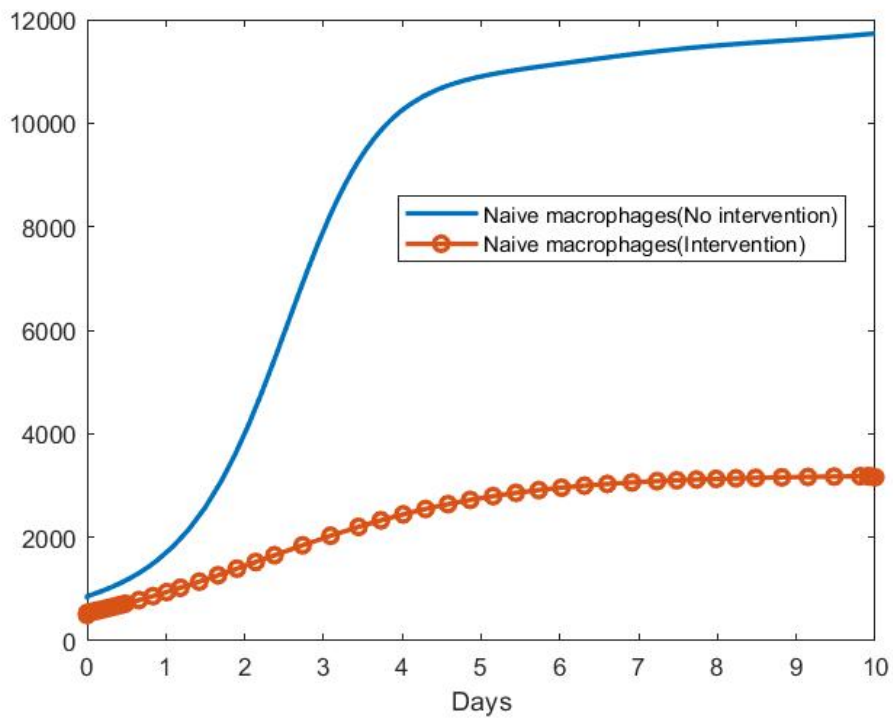
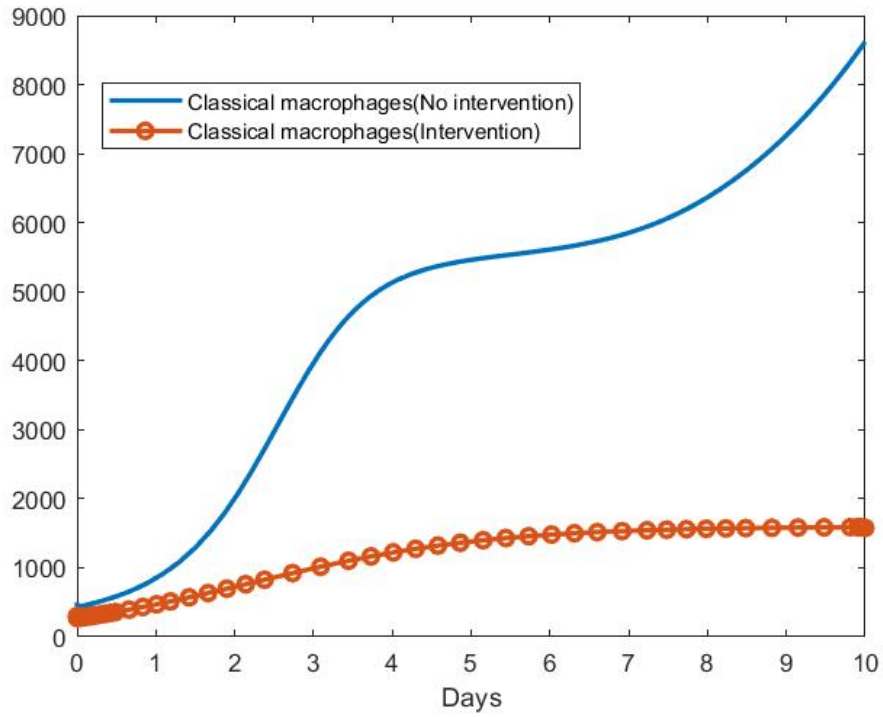
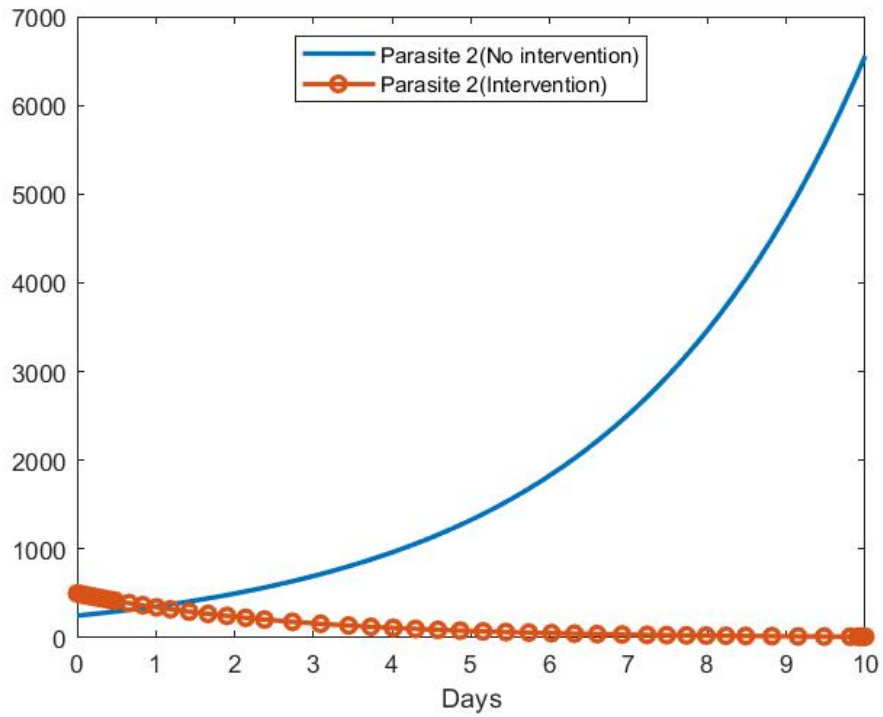


Figure 17: Numerical solutions of model system showing progression of naive macrophages with effects of second stage drug.



**Figure 18:** Numerical solutions of model system showing progression of classical macrophages with effects of second stage drug.



**Figure 19:** Numerical solutions of model system showing progression of parasite type 2 with effects of second stage drug.

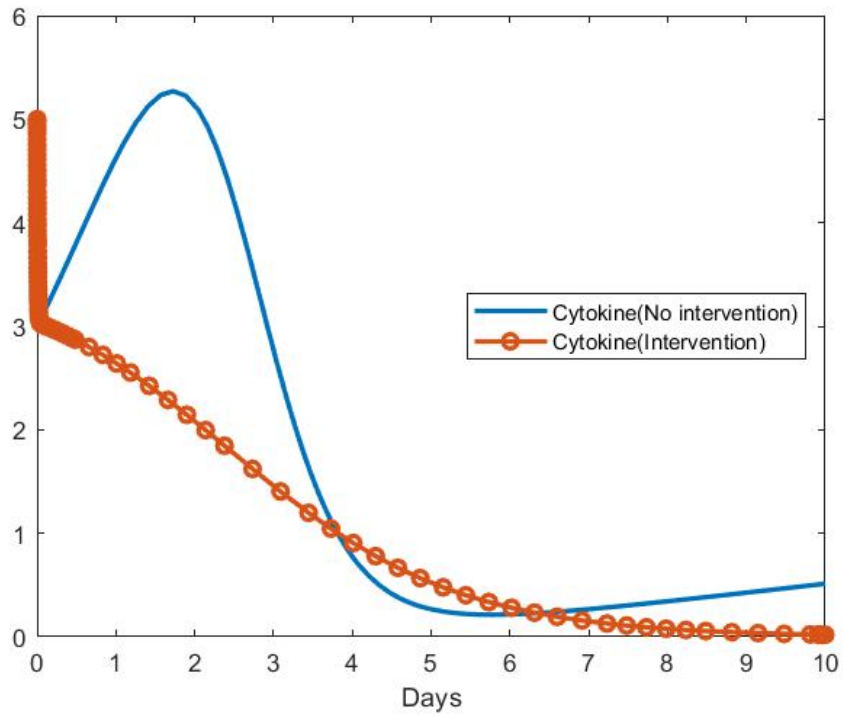


**Figure 20:** Numerical solutions of model system showing progression of cytokines with effects of second stage drug.

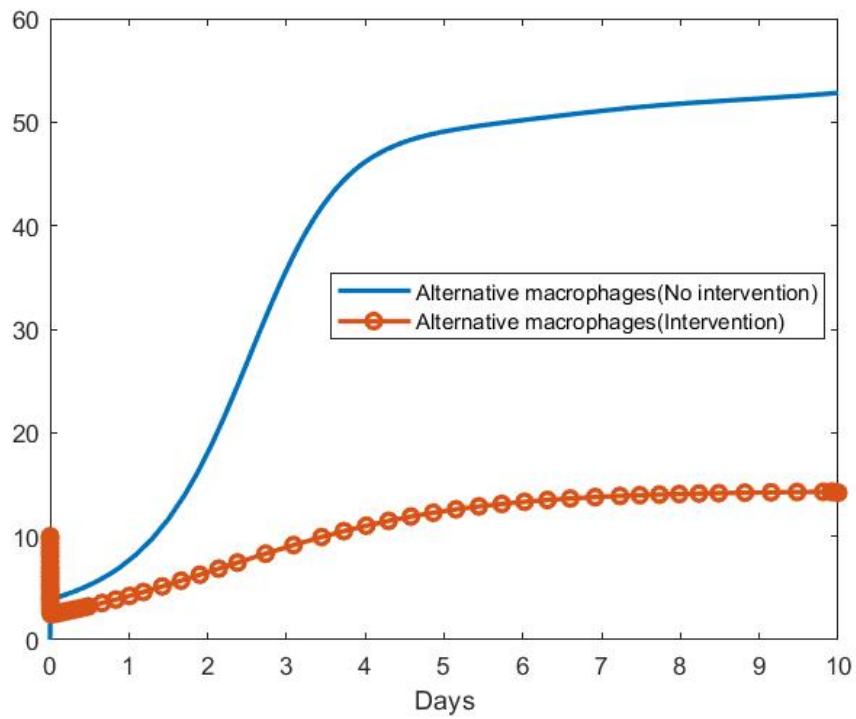


**Figure 21:** Numerical solutions of model system showing progression of alternative activated macrophages with effects of second stage drug.

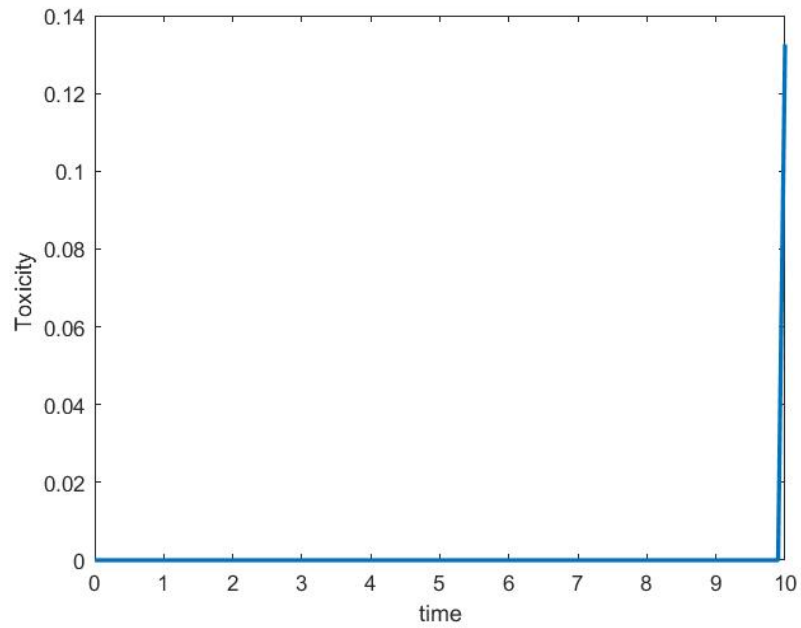


**Figure 22:** Numerical solutions of model system showing progression of alternative activated macrophages with effects of second stage drug.

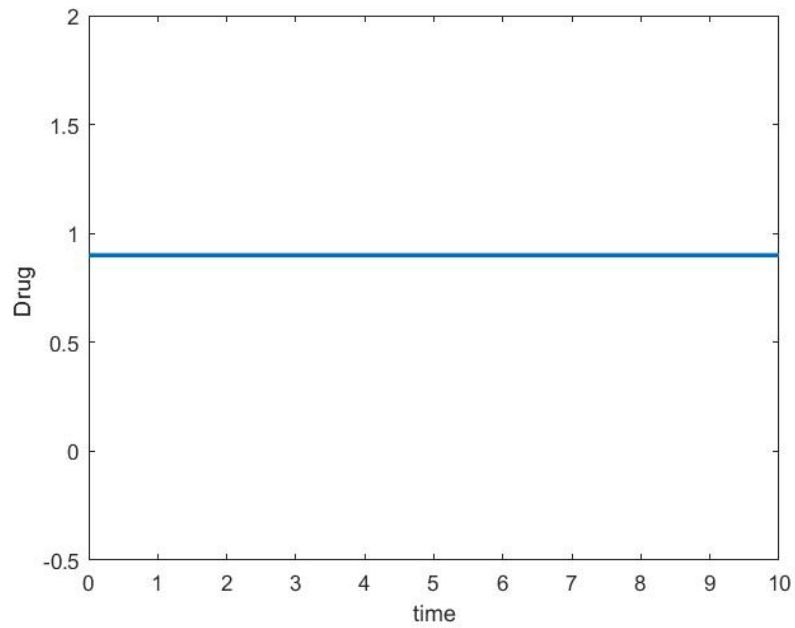


**Figure 23:** Numerical solutions of model system showing progression of alternative activated macrophages with effects of second stage drug.

the second parasite shows a decline over time in the presence of the second stage drug. In Figures 17, 18, and 21, we notice the drastic reduction in the macrophages, and that is due to the fact that the second stage drug is more toxic than the first stage drug.

From Figure 22, we notice the increase in the toxicity levels on the last day of treatment which explains drastic decline in the macrophages population. In this study we have discovered that for a drug to be efficient, the drug has to have an efficacy of 90% (see Figure 23). When a drug targets the population of the parasite at a given point it becomes difficult to control the parasite hence the rise on parasite type 2 still exist. In reality the parasite switches to multiple types of parasites, and in this paper we investigate using two types of parasites that.

## 6 Conclusion

The purpose of this study was to model and analyse the microscopic dynamics of the HAT disease within the human host. We obtained a system of six ordinary differential equations describing the switching of the parasite type 1 to type 2 and its interactions with various immune cells. There exist solutions to our system; the solutions are unique and positive. We performed a qualitative analysis of the system, and the analysis revealed the existence of one disease-free equilibrium state and two endemic equilibrium states. In addition, we carried out a stability analysis of the three equilibria using the Gershgorian circle theorem and van den Driessche and Watmough's method, and we established conditions of existence and stability of equilibrium states.

Furthermore, to investigate if the switching of the parasite from one type to the other helps the disease to persist within the host, numerical solutions of the system under consideration are presented. Figures 2, 3, and 4 show the solutions of the system of equations (1)–(6) without parasite switching. It can clearly be seen that in the absence of switching, the immune cells are able to clear the parasite from the body.

We then incorporate parasite switching in the system of equations (1)–(6). It can be observed in Figure 5 that the parasite evades the immune system even though an adaptive immune response is initiated through alternative activated macrophages, in order to deal with the new parasite type. A single switch reveals that the body is overwhelmed by the parasite load. This is indicated by the sharp increase in parasite type 2 after a few days of infection Figure 5, as well as the increase in alternative activated macrophages Figure 7. Naïve and classical macrophages are part of the innate immune system, while alternatively activated macrophages are produced when the innate system fails to fight parasites.

In the effort of clearing the parasite from the host, two optimal control models are introduced. The first controlled model shows cases of all possible HAT treatments that focus on the invasion of the parasite. This example is the case of Pentamidine, Suramin. These drugs specifically kill the parasite in the blood system. In the effort to find the optimal drug dosage and at the same time reduce the toxicity of the drug, our performance measure focuses on reducing the parasite load and finding the optimal final time. The controlled model is simulated numerically and presented in Figures 9–14. It can be observed that, even though the parasites load is reduced, this type of drugs are not efficient in curing the disease due to parasite switching. It was found that the drug steers the system from the co-existing parasites states to only the parasite type 2, the endemic state, considering that in this work the parasite only switches to one other parasite type, when in reality the parasite switches to thousand different types. Furthermore, we observe a decline in macrophages, suggesting that drug toxicity is the influencing factor in reducing macrophage load with time.

The second optimal control model include treatments of HAT that specifically targets the reproduction of the parasites within the host. This example, is the case of Melarsoprol, Eflornithine, and Fexinidazole. The numerical results show that these type of drugs are quite efficient in the treatment of HAT, and more adopted to deal with the switching of the parasite of other types (see Figures 16–21). The numerical solutions confirm that there is a possibility of achieving total elimination of the HAT disease when using a growth inhibitor drug.

## References

- Artzrouni, M. and J. P. Gouteux (1996). A compartmental model of sleeping sickness in central Africa. *Journal of Biological Systems* 4(04), 459–477. 208
- Baral, T. N. (2010). Immunobiology of African trypanosomes: need of alternative interventions. *BioMed Research International*, Article ID 389153. doi: 10.1155/2010/389153. 209
- Bejarano, D. A. O., E. Ibargüen-Mondragón, and E. A. Gómez-Hernández (2018). A stability test for non linear systems of ordinary differential equations based on the Gershgorin circles. *Contemporary Engineering Sciences* 11(91), 4541–4548. 215
- De Pellis, L. G. and A. Radunskaya (2000). A mathematical tumor model with immune resistance and drug therapy: an optimal control approach. *Journal of Theoretical Medicine* 3, 79–100. 221

- Etchegorry, M. G., J. P. Helenport, B. Pecoul, J. Jannin, and D. Legros (2001). Availability and affordability of treatment for human African trypanosomiasis. *Tropical Medicine & International Health* 6(11), 957–959. 216, 226
- Frank, S. A. (1999). A model for the sequential dominance of antigenic variants in African trypanosome infections. *Proceedings of the Royal Society of London. Series B: Biological Sciences* 266(1426), 1397–1401. 208, 209, 217
- Gervas, H. E., N. K.-D. O. Opoku, S. Ibrahim (2018). Mathematical modelling of human African trypanosomiasis using control measures. *Computational and Mathematical Methods in Medicine*, Article ID 5293568. doi: 10.1155/2018/5293568. 208
- Mhlanga, J. D., M. Bentivoglio, and K. Kristensson (1997). Neurobiology of cerebral malaria and African sleeping sickness. *Brain Research Bulletin* 44(5), 579–589. 216
- Mohamed, C. C., A. Eladdadi, and K. Mokni (2018). Activation of the immune response by cytokines and its effect on tumour cells. *Letters in Biomathematics* 5(2), S178–S200. 217
- Navarrete, D. J. (2019). Parasites, clocks, and immunity: a within-host mathematical model of human African trypanosomiasis [Doctoral dissertation, Princeton University]. *Princeton University Senior Theses*, <http://arks.princeton.edu/ark:/88435/dsp01ng451m33x>. 208
- Ndondo, A. M., J. M. W. Munganga, J. N. Mwambakana, C. M. Saad-Roy, P. Van den Driessche, and R. O. Walo (2016). Analysis of a model of gambiense sleeping sickness in humans and cattle. *Journal of Biological Dynamics* 10(1), 347–365. 208
- Pienaar, E. and M. Lerm (2014). A mathematical model of the initial interaction between Mycobacterium tuberculosis and macrophages. *Journal of Theoretical Biology* 342, 23–32. 217
- Pontryagin, L. S., V. G. Boltyanskii, R. V. Gamkrelize, and E. F. Mishchenko (1986). *The Mathematical Theory of Optimal Processes*. John Wiley & Sons, New York. 221, 227
- Rock, K. S., C. M. Stone, I. M. Hastings, M. J. Keeling, S. J. Torr, and N. Chitnis (2015). Mathematical models of human African trypanosomiasis epidemiology. *Advances in Parasitology* 87, 53–133. 208
- Rogers, D. J. (1988). A general model for the African trypanosomiasis. *Parasitology* 97(1), 193–212. 207, 208
- Rószler, T. (2015). Understanding the mysterious M2 macrophage through activation markers and effector mechanisms. *Mediators of Inflammation*, Article ID 816460. doi: 10.1155/2015/816460. 209
- Thieme, H. R. (1948). *Mathematics in Population Biology*. Princeton University Press. 211
- Turner, M. D., B. Nedjai, T. Hurst, D. J. Pennington (2014). Cytokines and chemokines: at the crossroads of cell signalling and inflammatory disease. *Biochimica et Biophysica Acta (BBA)-Molecular Cell Research* 1843(11), 2563–2582. 208
- Uniting to Combat Neglected Tropical Disease (2019). <https://unitingtocombatntds.org/ntds/human-african-trypanosomiasis>. 207
- Wamwiri, F. N., G. Nkwengulila, and P. H. Clausen (2007). Hosts of *Glossina fuscipes fuscipes* and *G. pallidipes* in areas of western Kenya with endemic sleeping sickness, as determined using an egg-yolk (IgY) ELISA. *Annals of Tropical Medicine and Parasitology* 101(3), 225–232. 207
- Wockner, L. F., I. Hoffmann, L. Webb, B. Mordmüller, S. C. Murphy, J. G. Kublin, P. O'Rourke, J. S. McCarthy, and L. Marquart (2020). Growth rate of *Plasmodium falciparum*: analysis of parasite growth data from malaria volunteer infection studies. *The Journal of Infectious Diseases* 221(6), 963–972. 217
- World Health Organisation (2019). <https://unitingtocombatntds.org/en/neglected-tropical-diseases/disease-directory/Sleeping-sickness/>. 207
- Zhang, J.M., and J. An (2007). Cytokines, inflammation and pain. *International Anesthesiology Clinics* 45(2), 27. 208